COOPER UNION FOR THE ADVANCEMENT OF SCIENCE AND ART

Midterm - Wind Turbine Design

ME-408: Computer Aided Engineering

Author:
NEIL SAWHNEY
ALEX LANDINEZ
KHUSHANT KHURARNA
BENJAMIN MEINER
CALDER LEPPITSCH

Professor:
PROFESSOR BONDI

February 16, 2024

CONTENTS

Midterm - Wind Turbine Design

ME-408: Computer Aided Engineering

I. Problem Statement

Our consultancy of mechanical engineering students has been tasked by Enercon to put forward the design of a new tower for their onshore 9.25 MW wind turbine. Our goal is to design and optimize the tower for minimum weight using Fintie Element Analysis.

II. Design Requirements

- The nacelle must be mounted 500 ft above the ground and has a weight of 200,000 lbf. The nacelle's center of mass is over the tower's central axis.
- The rotor consists of a hub and three blades and has a diameter of 450 ft. Each blade has a length of 215 ft and an average width of 17.9 ft. Each blade weighs 15,000 lbf and has a center of mass 71.7 ft from the root. The blades are offset from the central axis by 25 ft.
- The operating range of the turbine is between 6 and 12 rpm. The tower must be designed such that the natural frequencies of vibration lie outside this range. This is to avoid catastrophic failure in the scenario that one blade falls off and the tower-free end experiences a rotating unbalanced mass.
- The turbine will only operate up to wind speeds of 70mph, but wind speeds of up to 125mph can be expected in the extreme case.
- The temperature at the site ranges from -10 $^\circ F$ to 135 $^\circ F$.
- The base of the tower will be mounted to a concrete pile structure. The design of the concrete pile is not within the scope of this analysis, but it can be assumed we have rigid members to attach to the base of the tower.
- A minimum factor of safety of 1.65 is required for the strength of all materials, with an additional increase of 6 for any connection hardware. The tower must not buckle by a factor of 8 under any loading.
- The deflection of the tower must not exceed 1 foot under nominal loading conditions. In extreme weather, the deflection must not exceed 1.35 feet.

III. Design Assumptions

A. Material

The construction material for the tower is AISI 1020 Steel. (Properties from *Matweb Material Data Sheet*). It is a low-carbon steel that is inexpensive, easily manufactured, ductile and has a high yield strength.

Parameter	Magnitude
Density	0.284 lb/in^3
Tensile Yield Strength	50800 psi
Tensile Ultimate Strength	60900 psi
Modulus of Elasticity	27000 ksi
Poisson's ratio	.29

TABLE I: Material properties

B. Loading Calculations

Figure Figure III.1 shows all the forces to consider in the design of the tower. This section will go through several calculations to find these forces, and the next section will summarize the values for each of the forces.

To obtain the loading values for the wind pressure on the tower the following equation is used.

$$P_{wind} = \frac{1}{2} C_d \rho V^2 \tag{1}$$

P	Pressure on Surface
C_d	Drag Coefficient (depends on the shape of the object)
ρ	Fluid (Air) Density
V	Fluid Velocity

The drag coefficient varies based on the surface the air is impacting. For the blades, it is given that they have a drag coefficient of 0.85. To obtain the drag coefficient values for the tower and the nacelle, the Reynolds number of the flow was first calculated. The Reynolds Number equation is,

$$Re = \frac{\rho u L}{\mu} \tag{2}$$

Re	Reynold's Number
ρ	Density of Fluid
u	Velocity of Fluid
L	Characteristic Length of Object
μ	Dynamic Viscosity of fluid

This number was calculated for the range of wind velocities and fluid properties. Based on the maximum values and known literature references, the drag coefficient was calculated for both flow perpendicular and parallel to a cylinder representing the flow over the tower and nacelle respectively. The following summarizes the drag coefficients used. $C_{d,nacelle} = 0.8$ $C_{d,blades} = 0.85$ $C_{d,tower} = 0.9$

The density of air varies depending on the temperature. $\rho_{air} = 0.0811\ lb/ft^3$ at -10 $^\circ F$

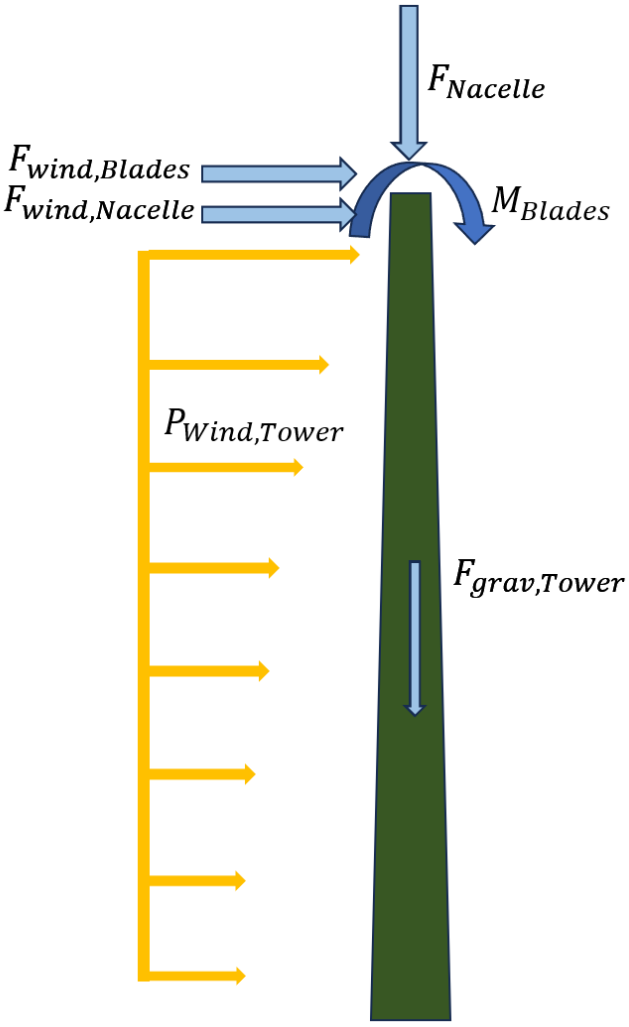

Fig. III.1: Schematic of Forces on Tower

$\rho_{air} = 0.0542\ lb/ft^3$ at 135 $^\circ F$ The wind speed is modeled using the wind profile power law for both extreme wind conditions and normal wind conditions. This is a commonly used estimate for how wind speed varies near the boundary layer of the earth's surface. It is represented by the relationship:

$$Vy^{-\alpha} = const.$$

Leading to the equation:

$$V(y) = V_{top}\left(\frac{y}{l}\right)^{\alpha} \tag{3}$$

V is the wind velocity, y is the distance from the ground, l is the length of the tower, and V_{top} is the wind velocity at the top of the tower. The term α is known as the Hellman exponent and is chosen as 0.3 for this case as we can assume this wind turbine is placed in the countryside with trees and shrubs [2]. The wind force on the blades is found using the following equation.

$F^{wind}_{blades} = n_{blades}A_{blade}P_{wind}$

The wind force on the nacelle is found using the following equation.

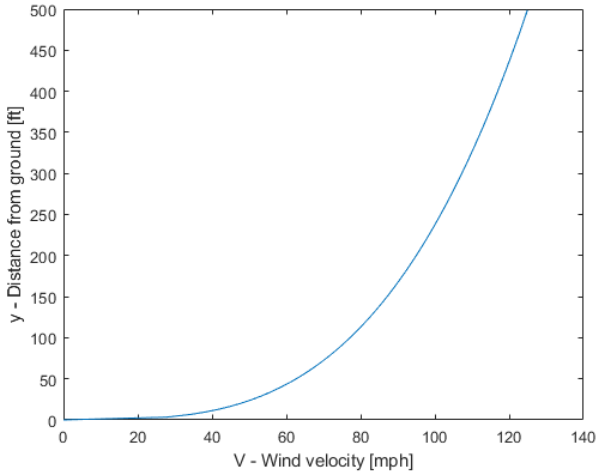

Fig. III.2: Wind Profile Power Law

$F^{wind}_{nacelle} = A_{nacelle}P_{wind}$

The wind pressure on the tower is calculated using the variable wind velocity as described in the section above applied as a pressure in each section of the tower. A more detailed description of these sections can be found in future sections.

C. Loading Results

The tower is subjected to a multitude of loading conditions in both nominal operation and extreme weather. The permanent loads are as follows (All loads are expressed in the coordinate system as shown in :

- Nacelle - 200,000 lbf applied axially in the -Y direction
- Blades - 45,000 lbf applied axially in the -Y direction
- Blades - 1,125,000 lbf-ft moment applied in the -X direction about the top surface of the tower.
- Gravity - Variable, depends on the tower geometry in simulation

The varying loads are due to temperature and wind fluctuations, and there are multiple cases for each. For temperature, it simply requires testing the two extreme temperature conditions. It is assumed that the material started at 68 $^\circ F$. For the wind loads, two operating conditions are assumed. First is the nominal operating condition with 70mph winds blowing into the rotor head-on, which resulted in the following values for wind loading:

- Blades - 130,569 lbf applied in the +Z direction at the top surface of the tower due drag of the wind on the blades.
- Nacelle - 3341 lbf applied in the +Z direction at the top surface of the tower due to the drag of the wind on the hub and nacelle.
- Tower - The distributed load from the wind on the tower varies with the height of the tower due to the wind profile power law model. At the top of the tower, the pressure with 70 mph winds is 0.0831 psi.

In extreme wind conditions of up to 125mph, the turbine will not be operational due to the danger of high spinning speeds leading to failure. In this case, the rotor head is not guaranteed

to be facing the wind and in the worst case, the wind will blow from the rear of the nacelle, adding to the moment created by the off-center blades. The higher speeds result in the following values:

- Blades - 416357 lbf applied in the +Z direction at the top surface of the tower due drag of the wind on the blades.
- Nacelle - 10653 lbf applied in the +Z direction at the top surface of the tower due to the drag of the wind on the hub and nacelle.
- Tower - The distributed load from the wind on the tower varies with the height of the tower due to the wind profile power law model. At the top of the tower, the pressure with 125 mph winds is 0.265 psi.

D. Factor of Safety

One of the design assumptions employed in the design process is an extra margin of error beyond the requirements given in the design prompt. This was to give the tower an extra degree of safety with regards to any unmodeled stress concentrations. For the stress in the steel, a minimum factor of safety of 2 is chosen instead of exactly 1.65, meaning the maximum stress at any point is less than 25400 psi. For the deflection of the tower a minimum factor of safety of 1.5 is chosen, meaning the tower does not deflect more than 0.66 ft.

E. Life Expectancy

The tower and base should be operational for at least 20 years[3]. A factor of safety of at least 1.5, resulting in a design objective of 30 years, is employed.

IV. Tower Design

The following section provides a detailed dive into the final decisions regarding the design of the tower.

A. Sectioning

The tower is sectioned into 8 cylindrical pieces of varying thickness and diameter to reduce material usage and aid in manufacturing. To hold each section together, a solid rectangular rib of cross section 3"x1' is wrapped in a circle on the inside ends of each cylindrical section and welded in place. The sections are then welded together through the ribs. For the remainder of the tower analysis, it will be assumed that the connection between each of the tower sections is rigid.

In Ansys Workbench, the design is implemented by attaching a beam with a 6"x1' rectangular cross-section to the intersection of each cylindrical shell section as shown in Figure IV.1.

B. Variable Section Thickness

Observing the stress plots from the FEA analysis of a constant thickness tower as shown in Figure IV.2, it can be seen that there is a stress concentration at around 10 times greater stress than the rest of the structure at the very bottom edge of the tower, and the stress gradually decreases up the tower. This effect is in part due to the fixed boundary constraint at the bottom which creates an artificially high stress at the boundary. Various techniques such as increasing the resolution of the mesh in this area or performing averaging near the boundary were implemented to mitigate the error, but ultimately it is difficult to decipher what portion of the stress at the boundary is real, and what is artificial. After utilizing error mitigating techniques, the remaining stress output is assumed to be correct to ensure the tower was not under-designed. While increasing the thickness of the metal and increasing the base diameter both minimize the maximum stress of the tower, it is wasteful to thicken or enlarge the entirety of the structure to address such a concentrated area. This inspired the decision[1] to gradually decrease the thickness of the metal as it approaches the top as shown in Figure IV.3.

The result is a structure with overall lower maximum stress while also using less material.

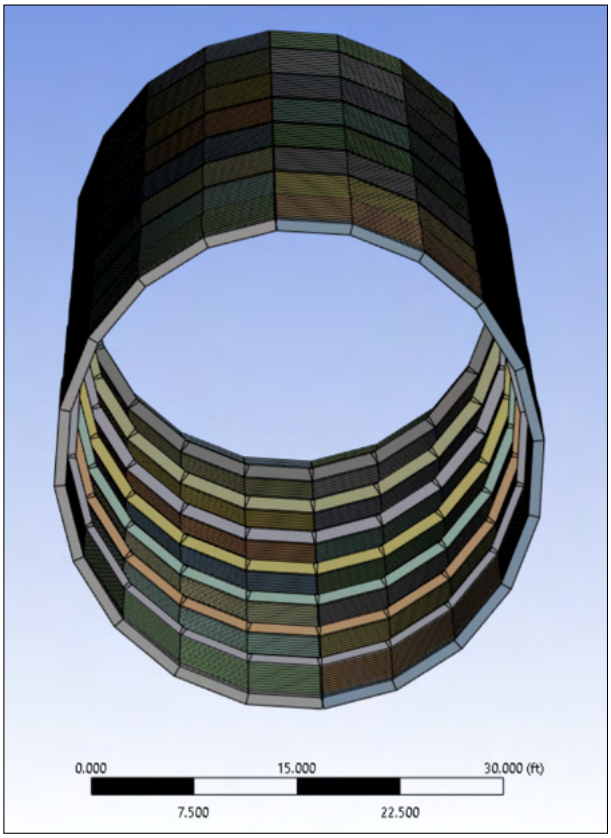

Fig. IV.1: Tower cylinder from below showcasing internal ribs. All beam elements have identical cross section; the apparent size difference is due to extreme perspective and orthographic projection.

C. Draft Ratio and Bottom Diameter

Decreasing the draft ratio, defined as $\frac{\text{Top Diameter}}{\text{Bottom Diameter}}$, or increasing the bottom diameter drives down the maximum stress and deflection. However, it also increases material usage. There arises an optimization problem that uses the

[1] An alternative solution to this problem which involves creating a fillet at the bottom of the structure is discussed in Appendix C-B

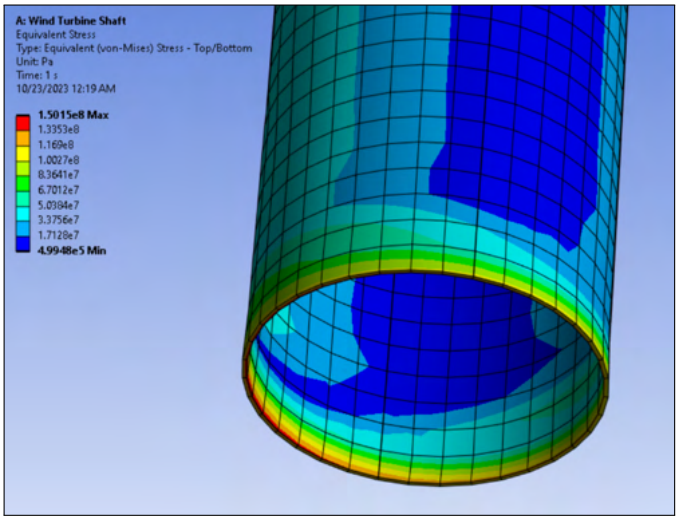

Fig. IV.2: Stress at the base of the tower before gradual thickening was implemented

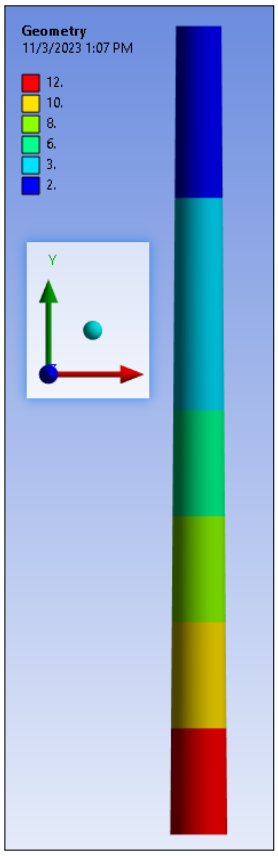

Fig. IV.3: Thickness of the tower sections in inches

least material usage while getting as close as possible to a minimum factor of safety of 2 for stress, and 1.5 for deflection in all operating conditions. Once reasonable values for each parameter are achieved, an enumeration solution search was performed in which every parameter is increased and decreased by a set interval until the resulting model failed the factor of safety criteria. Over 500 potential solutions are searched, resulting in an optimized draft ratio of 0.8, and a bottom diameter of 35 feet.

D. Weight

With this design, the volume of the tower is 25745 ft^3, corresponding to a mass of 12,634,410 lb. Estimating the cost is difficult, but it is reasonable to assume this tower will cost on the order of tens of millions of dollars to build. There is also reason to believe this tower's weight is not completely excessive. The GE Haliade X is a new wind turbine model entering the market with a tower length of 423 ft and has a mass of 5,622,000 lb [4]. A professional engineering firm like GE will have developed a highly optimized design, so it is reasonable that the design discussed here is twice as massive.

E. Scaled Sketches Illustrating the Conceptual Design

Detailed engineering drawings for the final design of the tower and base are shown in section A and section B respectively.

V. Verification Hand Calculations for Tower Design

To verify the deflection and stress values obtained in simulation, a MATLAB script is used to speed up the computation. For these calculations, a coordinate system is established with the origin at the intersection of the central axis of the tower and the bottom plane. The Y-axis points upwards along the central axis of the tower. The diameter of the tower at any point y as a function of the diameter at the bottom, top, and the length of the tower is expressed in Equation 4.

$$d(y) = d_b - \frac{y\ (d_b - d_t)}{l} \tag{4}$$

Although the tower thickness profile is a piecewise function of the tower height y with discrete stepped values, the thickness function is simplified for the hand calculation to a polynomial function to allow for easier integration. Equation 5 has a simple form and matches the section thicknesses closely. It takes in a height value y in feet and returns the thickness in inches.

$$t(y) = \frac{(y - 500)^2}{2000} + 2 \tag{5}$$

The cross sectional area of the tower at any point y is given in Equation 6, where $t(y)$ is the tower thickness function. In simulation, the shell element thickness is offset outwards from the diameter specification, resulting in a true outer diameter of $d + 2t$.

$$A(y) = \frac{\pi}{4}((d(y) + 2t(y))^2 - d(y)^2) \tag{6}$$

The tower's cross sectional moment of inertia about the neutral axis at height y is therefore:

$$I(y) = \frac{\pi}{64}\left((d(y) + 2t(y))^4 - d(y)^4\right) \tag{7}$$

The weight of the tower above any point y is given by Equation 8.

$$W_{tower}(y) = \rho_{\text{steel}} g \int_y^l A(\tilde{y}) d\tilde{y} \tag{8}$$

The distributed load normal to the tower surface due to wind at any point y along the length of the tower is given by Equation 9

$$\begin{aligned} w(y) &= p_{wind}(y)d(y) \\ &= 0.5C_{d,tower}\rho_{air}V_{top}^2\left(\frac{y}{l}\right)^{2\alpha}d(y) \end{aligned} \tag{9}$$

The total axial load applied to the tower at any point y is expressed as the sum of all vertical loads in Equation 10

$$P(y) = W_{nacelle} + W_{blades} + W_{tower}(y) \tag{10}$$

The total moment applied to the tower at any point y is given in Equation 11.

$$\begin{aligned} M(y) =& M_{blades} + (F_{nacelle}^{wind} + F_{blades}^{wind})(l-y) \\ &+ \int_y^l w(\tilde{y})(\tilde{y}-y)d\tilde{y} \end{aligned} \tag{11}$$

Using the axial load and moment equations, it is straightforward to solve for the stress and deflection at any point assuming that the deformation is elastic and the tower behaves like a beam. In reality the tower will not behave exactly like the beam as the thickness to diameter ratio of the cylinder is low, making it behave more like a shell. For the scope of this hand calculation however, the results should be a reasonable estimate. Stress from the applied moment varies throughout the cross section. In order to find the points of maximum stress, it is necessary to look at the edges of the cylinder furthest from the neutral axis. This corresponds to the lines of intersection between the cylinder and a Y-Z plane passing through the central axis. At these points, the stress can be expressed as a sum of components from the axial load and the bending moment as seen in Equation 12.

$$\sigma_y = \frac{P}{A} \pm \frac{M(d+2t)}{2I} \tag{12}$$

All the variables in this equation are functions of the distance from the ground y and were derived previously. Note that on opposite sides of the tower, the bending moment creates equal tensile and compressive stresses that combine with the inherently compressive stress of the dead loads.

The tower deflection is calculated using beam theory from Equation 13, where x is the deflection normal to the beam axis and y is the distance along the beam axis. E is the Modulus of Elasticity for the material.

$$\frac{\mathrm{d}^2x}{\mathrm{d}y^2} = \frac{M(y)}{EI(y)} \tag{13}$$

Integrating twice and making use of the boundary conditions of the base $\frac{\mathrm{d}x}{\mathrm{d}y}|_{y=0} = 0$ and $x(0) = 0$, Equation 14 is obtained for the deflection of the beam.

$$x(y) = \int\int \frac{M}{EI}\mathrm{d}y^2 - \int\int \frac{M}{EI}\mathrm{d}y^2|_{y=0} - y\int \frac{M}{EI}\mathrm{d}y|_{y=0} \tag{14}$$

With the current model of varying diameter and thickness as a function of height y, calculating the integral of $\frac{M(y)}{EI(y)}$ is very difficult. To simplify the process of finding a reference deflection value, it is necessary to assume a constant thickness and diameter for the entire tower. A median thickness of 6 inches and an average diameter of 31.5 ft is used to find the following values for the different load cases.

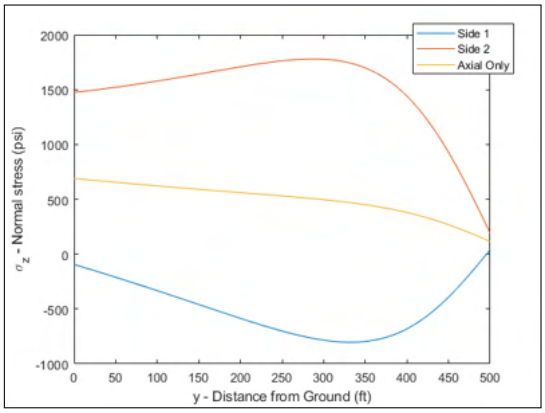

Fig. V.1: Stress on tower sides - Operational Loading

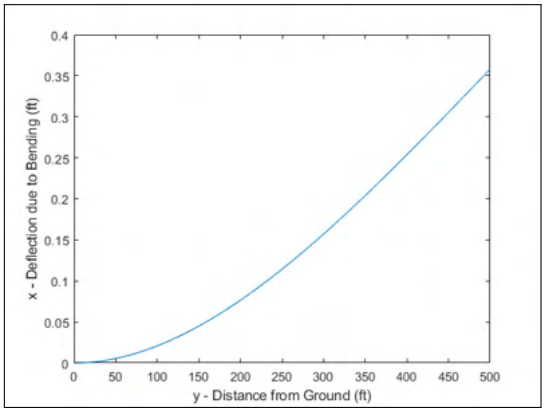

Fig. V.2: Tower Deflection - Operational Loading

A. Normal Loading

The operational loading condition is 70mph winds at a temperature of $68°F$.

1) Tower Stress: The calculated tower stress varies along the length of the tower as seen in Figure V.1. The maximum value is 1780 psi and occurs at the outer edge of the shell on the concave side of the tower bend at a height of 288ft.

2) Tower Deflection: The deflection increases with height. The maximum is 4.30 in, and occurs at the free end 500 ft high. The variation over the height can be seen in Figure V.2

B. Extreme Weather Event Loading

The extreme loading condition is 125mph winds at a temperature of $-10°F$. The lower temperature increases the density of air and the resulting wind pressure forces on the tower are larger.

1) Maximum Tower Stress: The maximum stress in the tower under extreme weather is 4,510 psi and occurs at 300ft. Once again the maximum stress is found on the outer edge of the concave bend side. The variation of the stress for this case can be seen in Figure V.3.

2) Maximum Tower Deflection: The maximum deflection in this case is 13.56 in and occurs at the free end. The extra factor of safety allowance provided for the extreme weather case is needed for this case. The deflection profile can be seen in Figure V.4

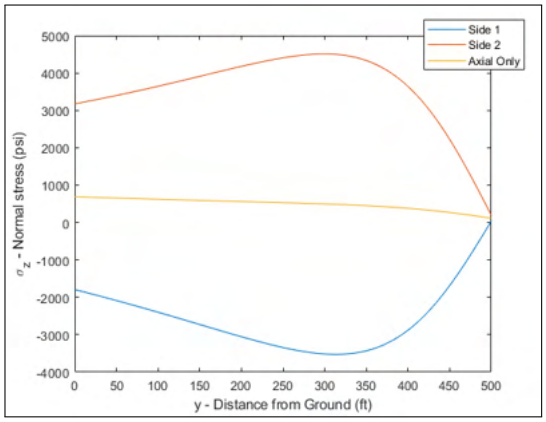

Fig. V.3: Normal stress along tower sides - Extreme Loading

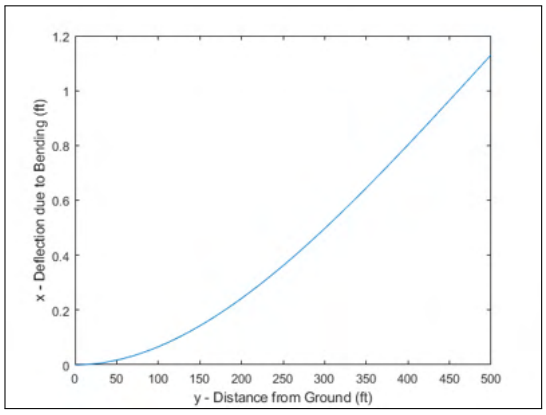

Fig. V.4: Tower Deflection - Extreme Loading

C. Change in Tower Height due to Temperature Differences

To find the change in tower height due to temperature differences, the equation for linear thermal expansion will be used. The equation is,

$$\Delta L = \alpha L_0 \Delta T \tag{15}$$

ΔL	Change in Length of Material
α	Thermal Expansion Coefficient
L_0	Original Length
ΔT	Change in Temperature of Material

The Coefficient of Thermal expansion for steel from *Engineering Toolbox* ranges from $6-6.94\frac{10^{-6}}{^\circ F}$. The value chosen is $6.7\frac{10^{-6}}{^\circ F}$ in accordance with the given value for structural steel in ANSYS with the original length of $500ft$. The change in temperature is considered for both extreme temperature cases and it is assumed that the standard temperature is $68^\circ F$. At the highest site temperature of $135^\circ F$, ΔT is $67^\circ F$. At the lowest site temperature of $-10^\circ F$, ΔT is $-78^\circ F$. Plugging in these values for the highest temperature yields,

$$\Delta L_{hot} = (6.710^{-6}\frac{1}{^\circ F})(500ft)(67^\circ F)$$
$$\Delta L_{hot} = 0.22ft$$

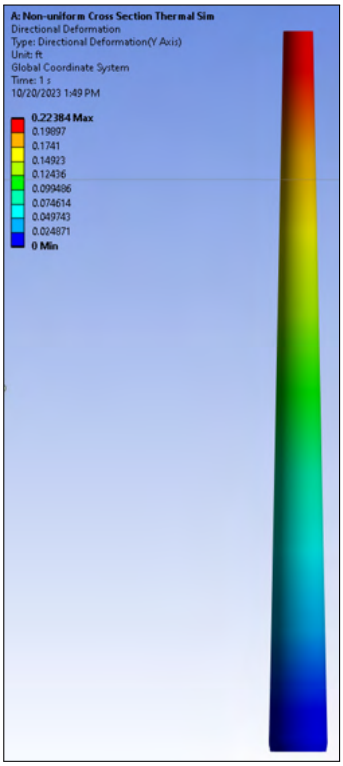

Fig. V.5: Thermal Expansion in the Vertical Direction in Hot Environment

For the lowest possible temperature this yields,

$$\Delta L_{cold} = (6.710^{-6}\frac{1}{^\circ F})(500ft)(-78^\circ F)$$
$$\Delta L_{cold} = -0.26ft$$

To confirm these values, they are compared to a simple ANSYS simulation looking at the thermal expansion using a hollow tube. It is created using a surface with a bottom diameter of 20 ft and a top diameter of 10 ft and specifying a shell thickness of 0.5 ft. A fixed condition is put on the bottom surface and a thermal condition is placed on the whole surface. Figure V.5 and Figure V.6 are the results for the hot and cold cases respectively.

A summary of the results is provided in Table II. As shown

	Hot Environment $(130^\circ F)$	**Cold Environment** $(-10^\circ F)$
Hand Calculations	0.22 ft	-0.26 ft
ANSYS Simulation	0.22 ft	-0.26 ft

TABLE II: Thermal Expansion Hand Calculations vs ANSYS Simulation Results

in Table II, the values match perfectly and confirm the hand calculations.

D. Blade Failure Natural Frequency

To find the natural frequency of the tower, the tower is modeled as a cantilever with a distributed force. The first

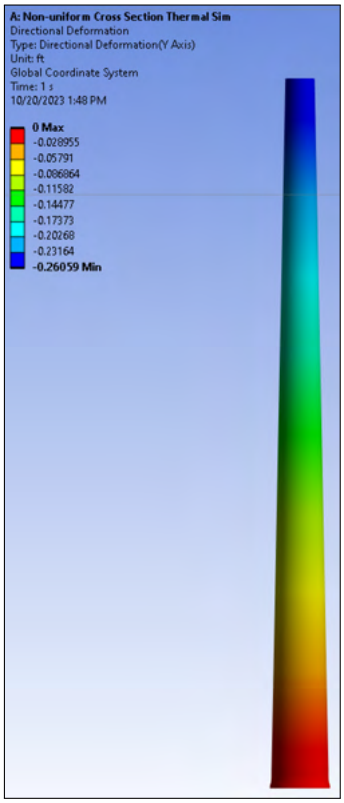

Fig. V.6: Thermal Expansion in the Vertical Direction in Cold Environment

natural frequency of a cantilever with a distributed force is described in Equation 16 from *Engineering Toolbox*.

$$f = 0.56\frac{EI}{qL^4}^{0.5} \tag{16}$$

E	Young's Modulus of the Material
I	Moment of Inertia of the Cross Section
q	Distributed mass
L	Length of the cantilever

The cross-section to be used is a hollow disk in which the diameter and thickness of the proposed design is averaged. The Young's modulus of structural steel, 186 GPa as discussed in subsection III-A, is used for E, and 500 feet is used for the length of the cantilever as discussed in section II. The distributed mass is calculated from the volume of a hollow cylinder.

The equation for the moment of inertia of a hollow disk about its centroid is shown in Equation 17 from the *Professional Engineer Mechanical Handbook*.

$$I_{y_c} = \frac{\pi(r^4 - (r-t)^4)}{4} \tag{17}$$

r	The outer radius of the disk
t	The thickness of the disk

After substituting the average width for a, and the average thickness for t from subsection IV-C and subsection IV-B respectively:

$$I_{y_c} = \frac{\pi * (33.25ft)^4 - ((33.25ft) - (5.33in))^4}{4}$$
$$I_{y_c} = 452,769ft^4$$

$$f = 0.56\frac{EI}{qL^4}^{0.5}$$
$$f = 0.56\left(\frac{(186GPa)(452,769ft^4)}{(868.14ft^2)(500ft)^4 * 7870\frac{kg}{m^2}}\right)^{0.5}$$
$$f = 0.82Hz = 49rpm$$

This result of 0.82 Hz or 49 rpm is well above the 6-12 rpm that the blades are spinning at. Therefore the tower is unlikely to fail due to resonance.

E. Tower Buckling

An estimate for the buckling factor can be found using Euler's Column formula.

$$F_{crit} = \frac{n\pi^2 EI}{L^2}$$

For this beam, the first buckling mode will be a quarter wave resulting in end condition term $n = 0.25$. The moment of inertia of the tower with respect to the neutral axis is not constant, so a simplification is required. For this calculation, the tower will be assumed to have a constant thickness of 6 in and diameter of 31.5 ft.

$$F_{crit} = \frac{0.25\pi^3(27 \times 10^6 psi)\left((378 + 12in)^4 - (378in)^4\right)}{64(500 \times 12in)^2}$$
$$F_{crit} = 2.47 \times 10^8 lbf$$

For the buckling factor calculation, the largest load currently applied axially to the tower is simply the weight of the tower itself.

$$BF = \frac{2.47 \times 10^8}{1.26 \times 10^7 + 200000 + 45000} = 19.2$$

To make this calculation more accurate, it would make sense to take a portion of the tower's weight as the axial loading condition. This would increase the buckling factor which is a positive outcome.

VI. Finite Element Analysis for the Tower

A. Mesh and Boundary Conditions

The final mesh uses shell elements, with an element count of 20 around every section intersection. From *ANSYS Mechanical APDL Element Reference*:

> SHELL181 is suitable for analyzing thin to moderately thick shell structures. It is a four-node element with six degrees of freedom at each node: translations in the x, y, and z directions, and rotations about the x, y, and z-axes.

Since the tower's surface is significantly larger in width and depth than thickness, the stress distribution across the thickness of the material is approximately uniform. Hence, a shell element is a suitable choice.

At each intersection there also exists a circular line meshed as beam elements with an element count of 20. From *ANSYS Mechanical APDL Element Reference*:

> BEAM188 is suitable for analyzing slender to moderately stubby/thick beam structures. The element is based on Timoshenko beam theory which includes shear-deformation effects. The element provides options for unrestrained warping and restrained warping of cross-sections.

The cross sections for each respective beam member are set based upon the decided-upon sections discussed in subsection IV-A.

It's important to note that according to *ANSYS Mechanical APDL Modeling and Meshing Guide*:

> The ROTZ degree of freedom of the shell element (the drilling mode) is associated with the in-plane rotational stiffness. This is normally a fictitious stiffness; that is, it is not the result of a mathematical calculation of the true stiffness; thus, the ROTZ degree of freedom of the shell element is not a true DOF. It is therefore inconsistent to connect only one node of a 3-D beam element to a 3-D shell element such that a rotational DOF of the beam element corresponds to the ROTZ of the shell element; beams should not be joined to shells in such a manner.

This, however, is not of major concern to us. The Z axis of each beam element will be approximately tangent to their respective shells and the ROTZ of each beam element is negligible for the small deflections that are being analyzed.

Mesh connections are used to connect the various sections with their respective neighbors and beams. The final mesh is shown in Figure VI.1. The beam connections and shell thickness' are shown previously in Figure IV.1 and Figure IV.3 respectively.

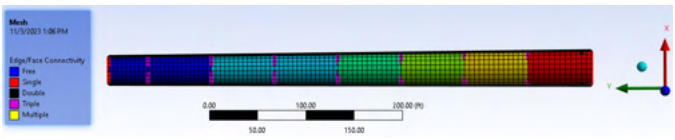

Fig. VI.1: Side view of the final tower mesh

	Nominal		Extreme	
Section	Wind (mph)	Pressure (psi)	Wind (mph)	Pressure (psi)
1	69.03	0.0808	123.28	0.2577
2	66.54	0.0751	118.82	0.2394
3	63.28	0.0679	113.00	0.2165
4	59.57	0.0602	106.38	0.1919
5	55.23	0.0517	98.63	0.1649
6	49.89	0.0422	89.10	0.1346
7	42.69	0.0309	76.24	0.0986
8	29.20	0.0145	52.14	0.0461

TABLE III: Pressure Variation with Height of Tower

All elements in the mesh pass element quality tests as shown in Figure VI.3.

The boundary conditions and loading used are shown in Figure VI.2

In order to create the variable wind profile, each section of the tower is assigned a different constant pressure which averaged the pressure value over the entire section. The values for each load case are detailed in Table III. The sections are numbered in order from the top of the tower to the base.

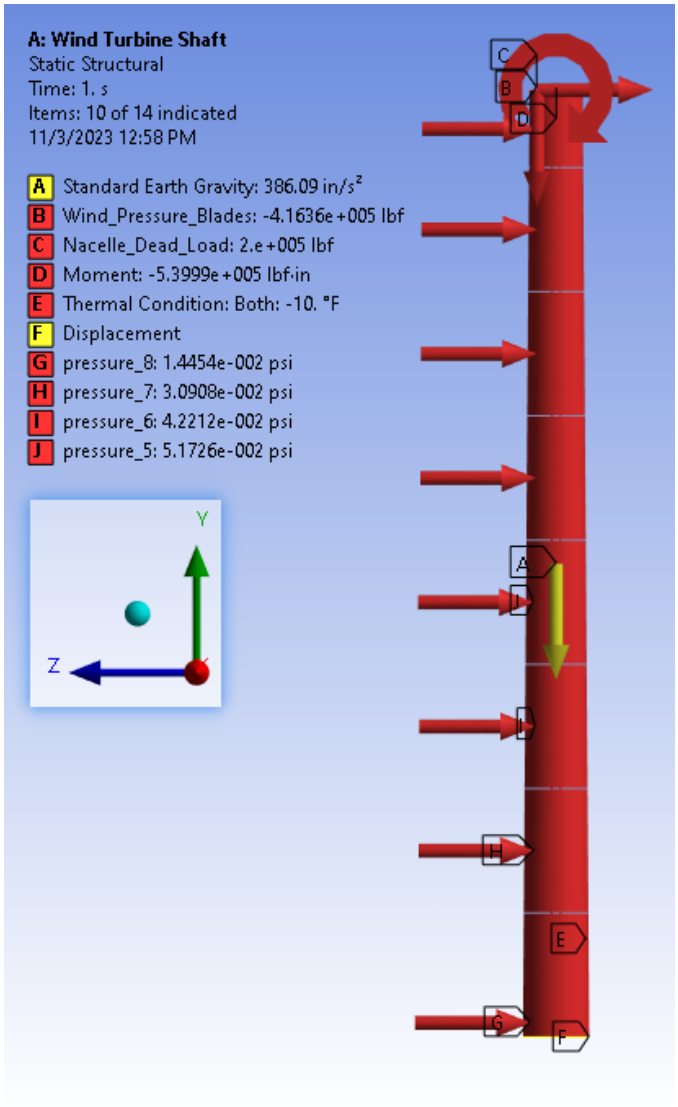

Fig. VI.2: Tower bounds and loads

Sheet | Solid

Error Check	Quality Criterion	Warning (Target) Limit	Error (Failure) Limit	% Warning	# Warning	% Failed	# Failed	Worst
☑	**Min Element Quality**	**Default (0.05)**	Default (0.02)	0 %	0	0 %	0	0.972
☑	Max Aspect Ratio	Default (5)	Default (1000)	0 %	0	0 %	0	1.143
☑	Min Element Edge Length	Default (6.417 in)	Default (0.642 in)	0 %	0	0 %	0	50.615 in
☑	Max Element Edge Length	Default (641.734 in)	Default (1283.469 in)	0 %	0	0 %	0	68.178 in
☑	Min Quad Angle	Default (30 °)	Default (10 °)	0 %	0	0 %	0	87.39 °
☑	Max Quad Angle	Default (150 °)	Default (170 °)	0 %	0	0 %	0	92.475 °
☑	Min Tri Angle	Default (20 °)	Default (10 °)	0 %	0	0 %	0	0 °
☑	Max Tri Angle	Default (160 °)	Default (170 °)	0 %	0	0 %	0	0 °
☑	Max Warping Angle	Default (20 °)	Default (30 °)	0 %	0	0 %	0	0.564 °

Fig. VI.3: Mesh Element Quality Analysis Results

Plots for the maximum deflection and stress of the tower are shown in Figure VI.4 and VI.5 respectively. Table IV displays the maximum stress, deflection, and their associated factor of safety for each case.

CONDTIONS	Equivalent Stress Maximum [Psi]	Total Deformation Maximum [in]	FOS - Deflection	FOS - Stress
Normal: COLD	18184.60	8.05	1.49	1.99
Extreme: HOT	14069.63	10.04	1.62	2.58
Extreme: COLD	18607.56	10.17	1.59	1.95
Normal: HOT	13665.46	7.75	1.55	2.65

TABLE IV: Tower Stress and Deformation for all Weather Conditions

	Hand Calculation		Simulation
Conditions	Maximum Stress (psi)	Maximum Deflection (in)	Max Stress (Neglecting Stress Concentration) (psi)
Normal	1780	4.3	2,150
Extreme	4,510	13.56	3,812

TABLE V: Comparison of Hand Calculations to Simulation

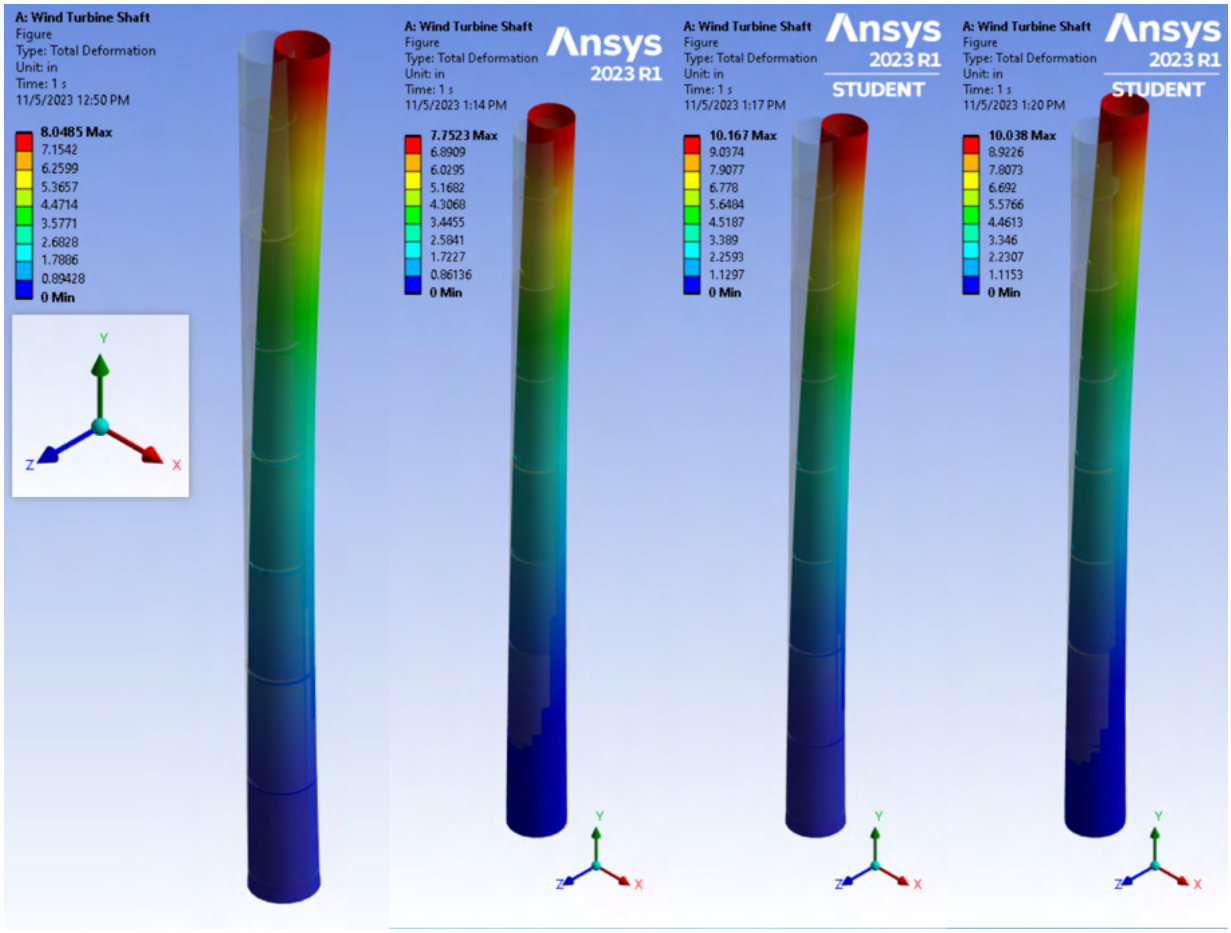

(a) Normal: -10 $^\circ F$ (b) Normal: 135 $^\circ F$ (c) Extreme: -10 $^\circ F$ (d) Extreme: 135 $^\circ F$

Fig. VI.4: Deflection of Tower in Various Weather Conditions. Normal refers to daily expected wind loads, and Extreme refers to hurricane conditions.

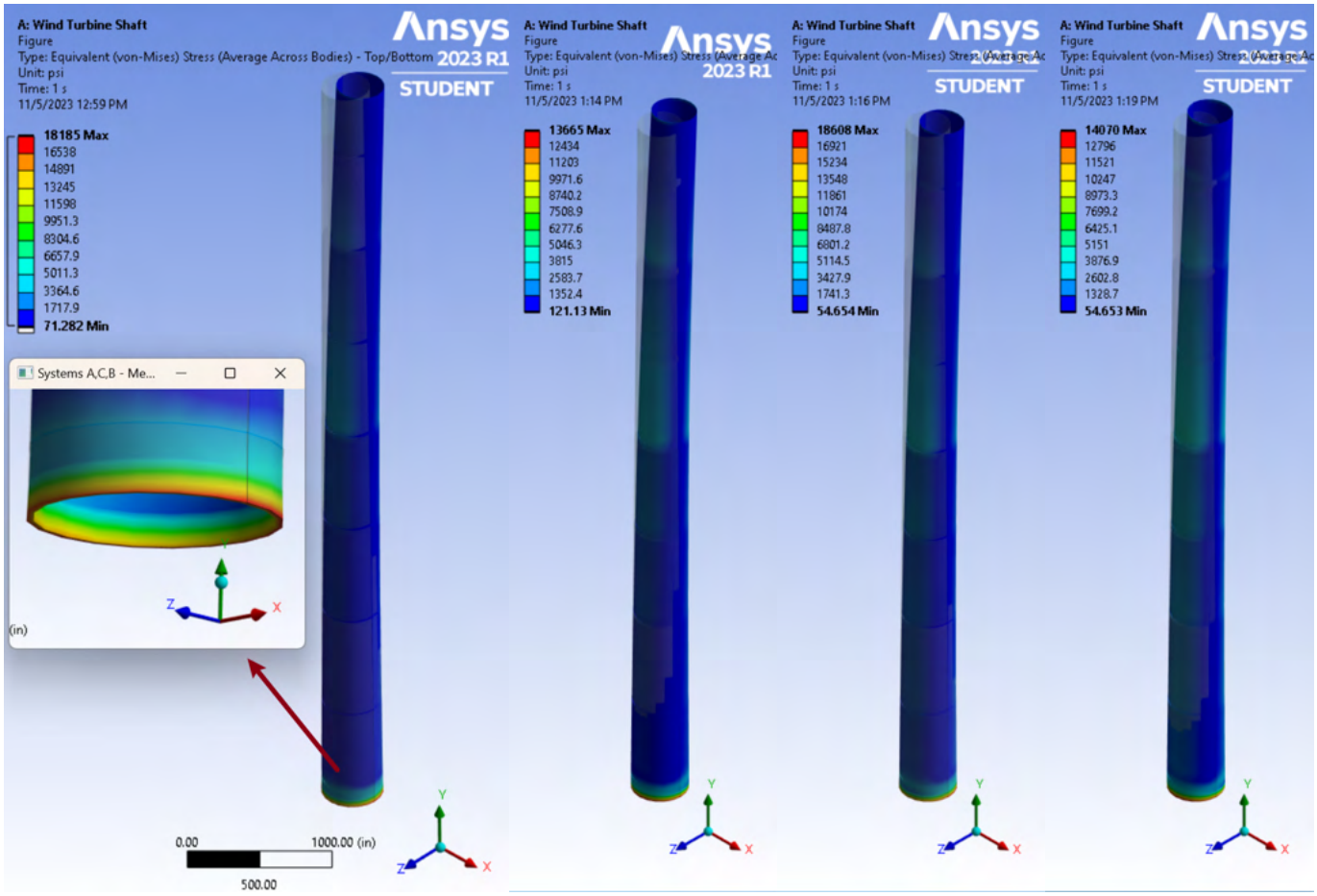

(a) Normal: -10 $^\circ F$ (b) Normal: 135 $^\circ F$ (c) Extreme: -10 $^\circ F$ (d) Extreme: 135 $^\circ F$

Fig. VI.5: Stress of Tower in Various Weather Conditions. Normal refers to daily expected wind loads, and Extreme refers to hurricane conditions.

B. Maximum Tower Deflection

The maximum deflection of the tower is 10 inches for the -10 $^{\circ}F$ case under extreme wind conditions as shown in Table IV. This corresponds to a factor of safety of 1.6. Despite this the case with the lowest factor of safety is the -10 $^{\circ}F$ case under normal wind conditions because of the lower deflection requirement, it has a maximum deflection of 8 inches and a factor of safety of 1.5. This is perfectly aligned with the design objective of a factor of safety of 1.5 for deflection as stated in section II. This deflection value matches well with the maximum tower deflection under extreme weather of 13.56 inches predicted by the hand calculation.

C. Maximum Tower Stress

The maximum stress of the tower is 19,000 psi for the -10 $^{\circ}F$ case under extreme wind conditions as shown in Table IV. This corresponds to a factor of safety of 2.0. The factor of safety for the -10 $^{\circ}F$ case under normal wind conditions also is 2.0. This is perfectly aligned with the design objective of a factor of safety of 2 for stress as stated in section II. The maximum stress is an order of magnitude larger than expected from the hand calculation. This is a product of the artificial stress concentration at the base of the tower. Looking further up the tower in Figure VI.10, the stresses along the side of the tower are closer in magnitude to the hand calculation prediction.

D. Factor of Safety Against Buckling Failure

The factor of safety against buckling is shown in Table VI for the first 5 modes. Their associated shapes are shown in Figure VI.6. The lowest factor of safety is 40 which is well above the requirement of 8 as stated in section II. This is also on the same order of magnitude as the factor of safety of 20 calculated in the hand calculation verification's.

	Mode	Load Multiplier
1	1.	42.528
2	2.	42.575
3	3.	73.919
4	4.	74.06
5	5.	136.1

TABLE VI: Tower buckling factor of safety table

E. Resonance Analysis

The natural frequency of the tower is shown in Table VII for the first 5 resonant modes. Their associated shapes are shown in Figure VI.7.

The first two modes are 0.84 Hz or 50.46 rpm which aligns well with the hand calculation of 0.82 Hz or 49 rpm as calculated in subsection V-D. Modes 3 and 4 are at around 3 Hz, or 180 rpm. All analyzed modes are well above the 6-12 rpm vibrations that are expected during a single or double-blade failure. The trend for higher modes is upwards in rpm which adds an additional layer of assurance that the tower will not fail due to resonance in the event of a single or double-blade failure.

	Mode	Frequency [Hz]
1	1.	0.84344
2	2.	0.84349
3	3.	2.9043
4	4.	2.9045
5	5.	3.6757

TABLE VII: Tower natural frequency table

F. Fatigue Analysis

In the fatigue analysis for the tower, the weight and moment of the nacelle load are suppressed because it will be placed once and never removed. The loading cycle is chosen to simulate wind gusts and therefore a full reversal loading cycle is chosen as shown in Figure VI.8.

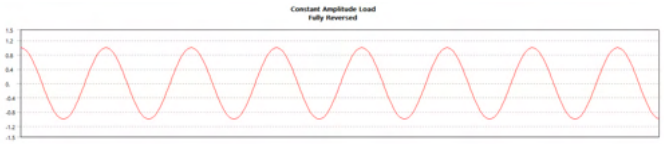

Fig. VI.8: Fatigue Loading for Tower

Over the duration of a day, it is assumed that the wind would make a full reversal every 20 minutes for a conservative analysis. After running the simulation, an estimated life cycle of 80 years is obtained during normal operating conditions. This results in a factor of safety of 4 for meeting its 20 year life expectancy.

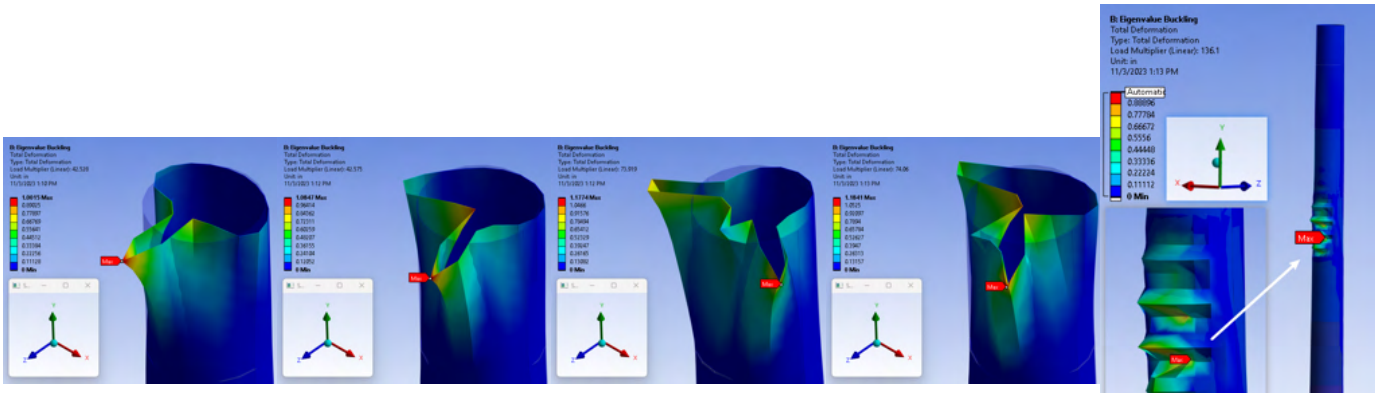

(a) Mode 1 (b) Mode 2 (c) Mode 3 (d) Mode 4 (e) Mode 5

Fig. VI.6: Tower Buckling Modes

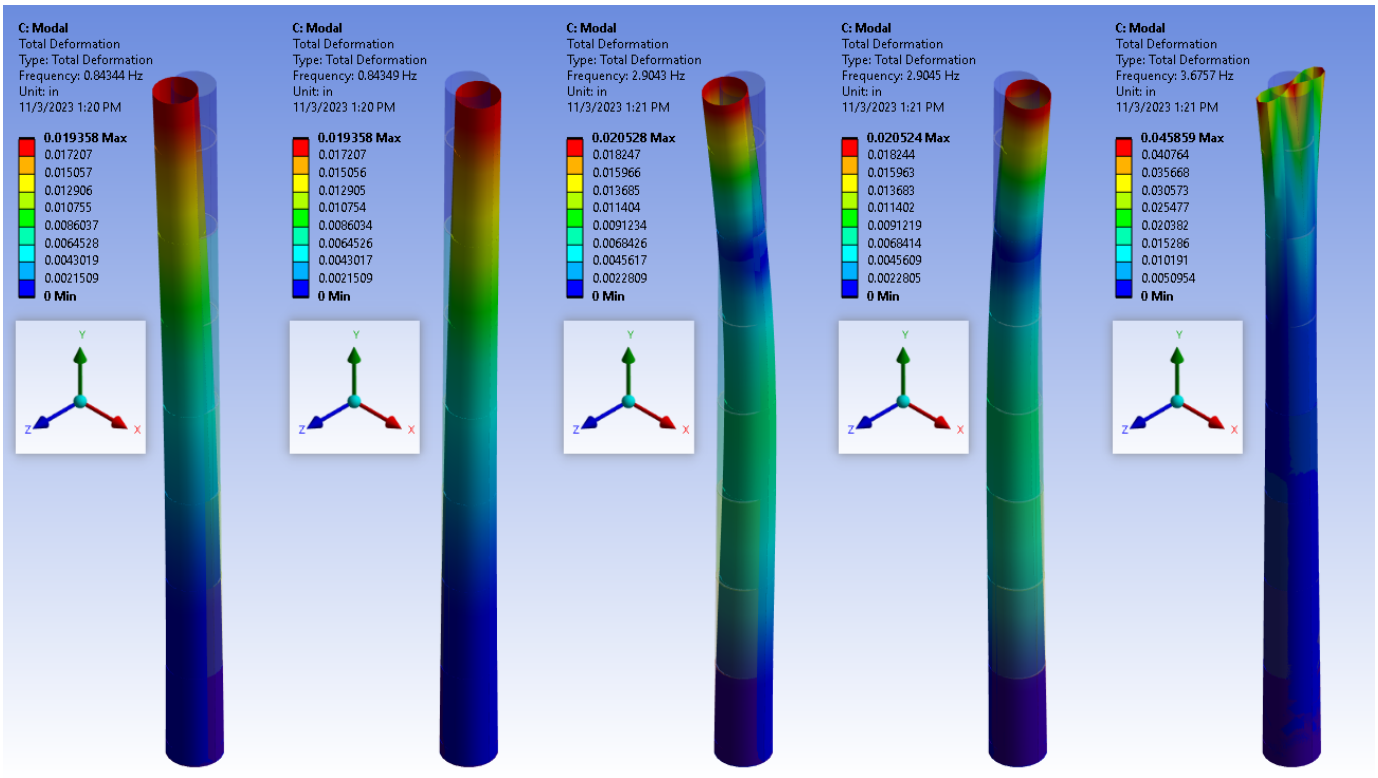

(a) Mode 1 (b) Mode 2 (c) Mode 3 (d) Mode 4 (e) Mode 5

Fig. VI.7: Tower Resonant Modes

G. Weld Analysis at Connections

To ensure that the welds connecting the tower section are strong enough, *Shigley's Mechanical Engineering Design* is used as a guideline to determine if the maximum stress in the welded locations are too high. A butt weld can be used as a secure connection between the tower layers. Using table 9.3 and 9.4 in *Shigley's Mechanical Engineering Design* as shown in Figure VI.9, an electrode number and strength can be chosen such that the design requirements are met. If an E90xx electrode is used, its yield strength is 77 ksi. Allowing for a factor of safety of 6 means that the design cannot exceed a yield strength, $S_y = 12.8ksi$. Using Table 9.4, it can be seen that the permissible stress for various loadings varies. For all except steering loading which is not applicable, the minimum permissible stress is $0.6S_y$. This means that our permissible stress is, $0.6 * 12.8ksi = 7.68ksi$ As shown in Figure VI.10, the maximum Von-misses stress in the welded areas is $3.5ksi$ which is less than the permissible stress of $7.68ksi$ which means the welds will be strong enough and have a factor of safety.

Table 9–3
Minimum Weld-Metal Properties

AWS Electrode Number*	Tensile Strength kpsi (MPa)	Yield Strength, kpsi (MPa)	Percent Elongation
E60xx	62 (427)	50 (345)	17–25
E70xx	70 (482)	57 (393)	22
E80xx	80 (551)	67 (462)	19
E90xx	90 (620)	77 (531)	14–17
E100xx	100 (689)	87 (600)	13–16
E120xx	120 (827)	107 (737)	14

*The American Welding Society (AWS) specification code numbering system for electrodes. This system uses an E prefixed to a four- or five-digit numbering system in which the first two or three digits designate the approximate tensile strength. The last digit includes variables in the welding technique, such as current supply. The next-to-last digit indicates the welding position, as, for example, flat, or vertical, or overhead. The complete set of specifications may be obtained from the AWS upon request.

Table 9–4
Stresses Permitted by the AISC Code for Weld Metal

Type of Loading	Type of Weld	Permissible Stress	n*
Tension	Butt	$0.60S_y$	1.67
Bearing	Butt	$0.90S_y$	1.11
Bending	Butt	$0.60\text{–}0.66S_y$	1.52–1.67
Simple compression	Butt	$0.60S_y$	1.67
Shear	Butt or fillet	$0.30S_{ut}^{\dagger}$	

Fig. VI.9: Butt Weld Strength for Various Electrodes and Types of Loading

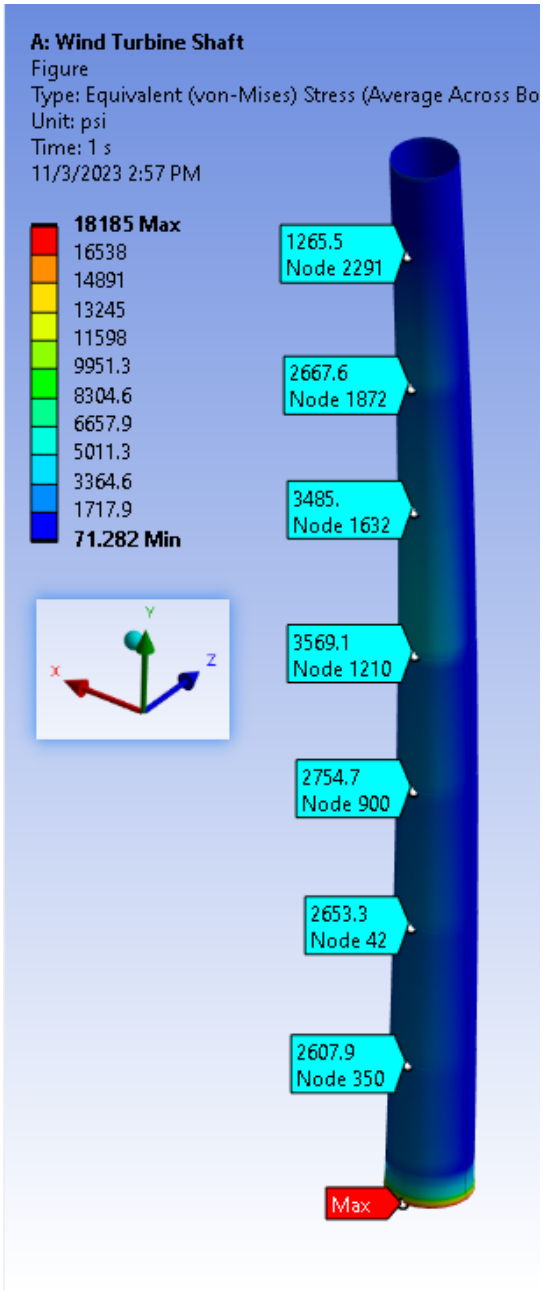

Fig. VI.10: Maximum Stress at Every Section Connection during Normal Loading at -10 $^{\circ}F$

VII. Base Plate Design

A. Design Iterations

The base plate design is replicated as a continuation of the tower by giving a small height and having the loads applied on top of that extrusion. Similar to real-world designs, the base plate includes bolts, flanges for the bolts to go on, and side supports for increasing the structural rigidity. Structural steel is used as the material for all iterations. In order to attain a factor of safety of 6 for the hardware and 1.5 for the structure itself, design parametrization is performed on three different designs: a single flange with 1 layer of bolts (Figure VII.1), a single flange with 2 layer of bolts (Figure VII.2), and two flanges with single layer of bolts each (Figure VII.3).

Each design is further parameterized by the number of bolts, bolt size, number of side supports, and the overall geometry. After analyzing all the designs, the base plate with 2 flanges with a single layer of bolts each is chosen as the final design. Table VIII shows the changes made across all the designs. The analysis conducted before rejecting the first two designs is shown in the Figure C-B

	Number of Bolts	Bolt Diameter	Number of side supports
Design 1	52	6 in	12
Design 2	258	2 in	12
Design 3	234	3 in	24

TABLE VIII: Major Design Changes Across Designs

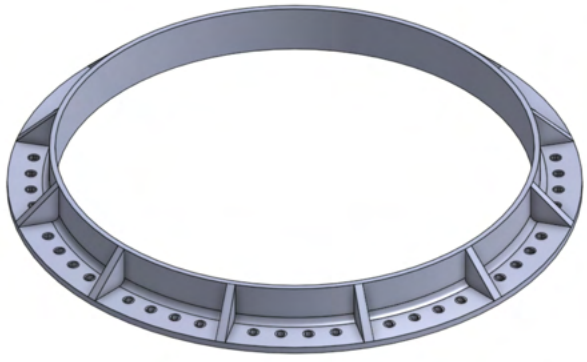

Fig. VII.1: First Base Plate Design With One Layer of Bolts

B. Deign of Bolt Hole With Respect to Thermal Expansion of the Base Plate

The bolt holes in the base are designed to allow for thermal movements. When the base heats up, the base will expand radially outwards. If the holes are designed with a circular hole then it will begin to sheer the stud bolt in the concrete. To get rid of this sheering force, the bolt hole is designed with a slot as shown in Figure VII.4

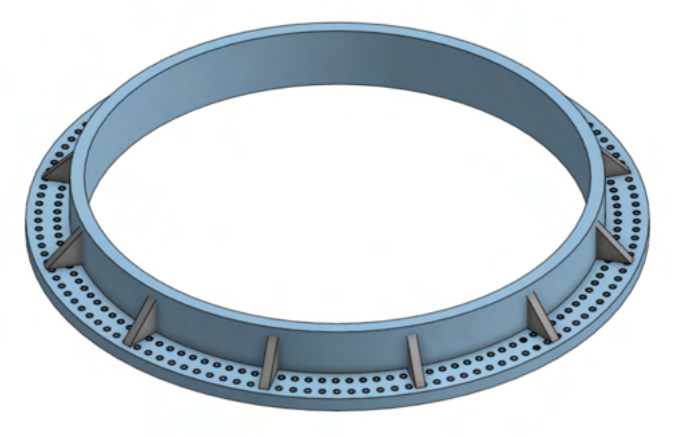

Fig. VII.2: Second Base Plate Design With One Flange and Two Layer of Bolts

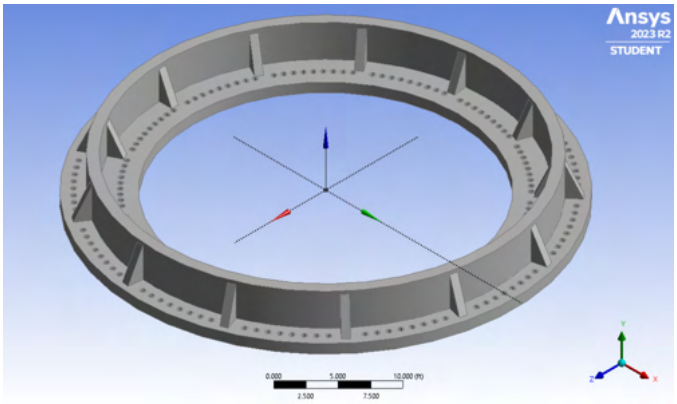

Fig. VII.3: Base Plate's Final Design: Two Flanges with Single Layer of Bolt Each

Fig. VII.4: Designing the Bolt Hole With Slot to Account for Thermal Expansion

To calculate the slot length, the thermal expansion can be calculated of the base. The base can be treated as a ring and since the thermal expansion at the bolt is of most importance it will be evaluated as a ring of a $20ft$ radius. To find the radial change of a ring of a certain radius, a similar equation to Equation 18 can be used and substituting length L for radius R.

$$\Delta R = \alpha R_0 \Delta T \tag{18}$$

ΔR	Change in Radius of Material
α	Thermal Expansion Coefficient
R_0	Original Radius
ΔT	Change in Temperature of Material

With a Radius of $20ft$, a temperature variation between -10 to $130°F$, and an α of $6.7\frac{10^{-6}}{°F}$ the equation evaluates to,

$$\Delta R = (6.710^{-6}\frac{1}{°F})(20ft)(140°F)$$
$$\Delta R = 0.019ft$$

To confirm this value in ANSYS a simplified flange model can be created without holes flanges. To simplify the model only a quarter of the model is necessary and symmetric boundary conditions can be made by constraining the movement perpendicular to the symmetry faces. The boundary conditions will be as follows. A thermal condition on the whole body with a base temperature of $-10°F$ and a current temperature of $130°F$ (This will result in the total radial change between the minimum and maximum temperatures). As shown in Figure VII.5, the maximum expansion is $0.019ft$, however where the bolts will be placed the expansion is about $0.018ft$. This value is close to the calculated value above of $0.019ft$ and the results are confirmed.

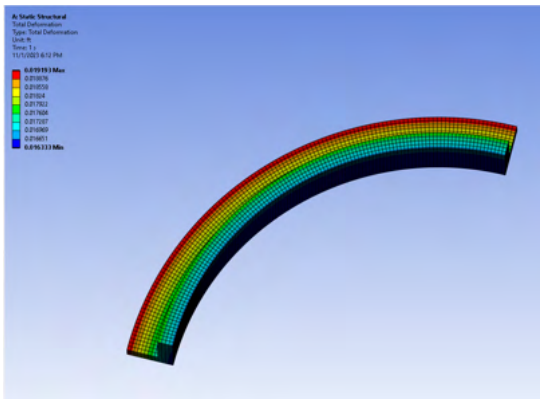

Fig. VII.5: Total Deformation of Base from Maximum Thermal Changes (-10 to 130 $°F$)

A slot length of $0.1ft$ is chosen for this design to build in a factor of safety that also accounts for installation error of the threaded studs in the ground.

C. Applied Loads and Constraints

Since the base design acts as a continuation of the tower, the reaction forces are derived from the base of the tower design (where constraint is applied) and are applied on the top of the base plate. In doing so, the signs are flipped because reaction forces are internal, and hence their direction needs to be flipped.

In order to apply the loads, "remote force" is used in order to supply the load evenly over the entire actuation and set the application point to be the middle of the extrusion since that mirrors the actual load application. The worst-case loading scenario, normal loading with extreme cold temperatures, as shown in Table IX is used for analysis. "Compression Only Support" is used to constrain the bottom of the base plate since it is in contact with the concrete, which is considered to be rigid. Accordingly, the reaction force generated from the ground would only come into play when the base plate is being compressed which models the actual scenario.

	Forces (lbf)	Moments (lbf*in)
X	-1152.3	-4541441751
Y	-12716600.0	-3009.6
Z	-980794.0	7012072.9

TABLE IX: Worst Case Forces and Moments Applied on the Base Plate (Normal Loading in Extreme Cold Weather)

To constrain the bolts, "fixed constraint" is applied to the bolt head because as the bolt is torqued into the ground, the only thing providing rigidity to the base is the bolt head. In other terms, the bolt head is fixed. A visual representation of the loads and constraints applied is shown in Figure VII.6. The team also analyzed the structure with "Compression Only Support" on the bolt head and the hole itself which yielded a result with negligible change.

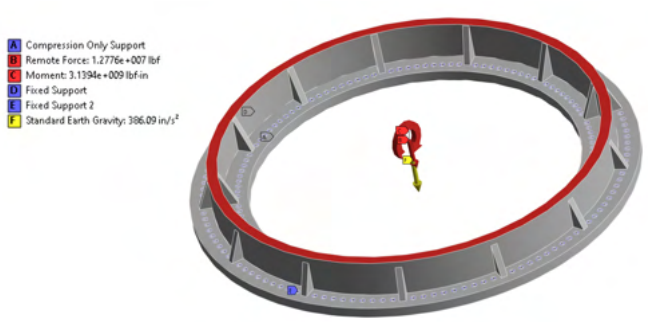

Fig. VII.6: Loads and Boundary Conditions Applied

D. Mesh Generated

"Patch Conforming Method" is used to generate a "Tetrahedron" mesh with an element size of 1.5 in. "Refinement" is added to the flanges and bolt heads because that is where the maximum stress occurs. An isometric view of the final mesh used is shown in Figure VII.7 and a close-up of the flanges and the bolt heads is shown in Figure VII.8. For conducting earlier analyses a dummy mesh with coarse elements is used to make post-processing faster. The metrics related to the final mesh quality are shown in Table X. The average element quality is around 0.75. The team tried to improve this by using "faced meshing" and playing with the element size, however, the results were similar. Finally, the skewness of the mesh is around 0.38 which also didn't change with different methods.

E. Post-processing

Since the loads applied by the wind and the nacelle bend the tower in one direction, the base plate is prone to compression and tension. While in compression, the bolts and the concrete underneath constrain the structure and provide rigidity. While in tension, however, only bolts constrain the structure because

Fig. VII.7: Final Tetrahedral Mesh Generated

Mesh Metric)	Magnitude
Total Number of Nodes	2551583
Element Size	1.5 in
Total Number of Elements	1620882
Average Aspect Ratio	2.18
Average Element Quality	0.73
Average Jacobian Ratio	0.986
Average Skewness	0.37
Average Minimum Element Edge Length	1.35
Average Maximum Element Edge Length	2.31

TABLE X: Mesh Metrics

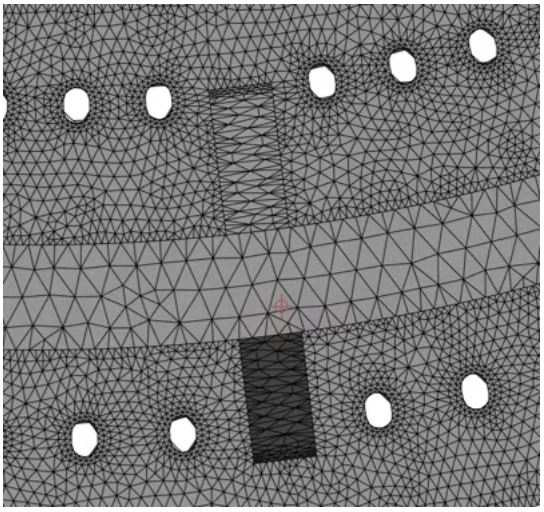

Fig. VII.8: Refinement Added Around the Bolt Holes and on the Flange

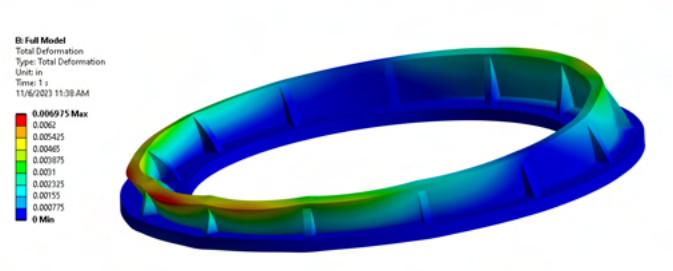

Fig. VII.9: Total Deflection (inches)

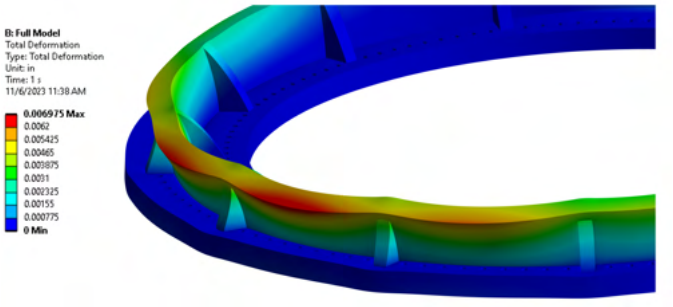

Fig. VII.10: Close up of total deflection (inches)

the ground support is modeled as ”compression-only support” which is not in contact with the plate anymore. Accordingly, the base design has a higher probability of failure under tension rather than when in compression which is also proven in the following analysis.

For all iterations made on the 3 designs, deflection is almost negligible however the structure fails in terms of stress or factor of safety for the hardware. The maximum deflection occurs at the extrusion which makes sense because that resembles the bottom part of the cantilever beam which is not constrained and the plate connection itself is constrained through bolts. The final deflection is determined to be 0.0069 inches which is less than the tower itself which also makes sense because the bottom part of the tower is closest to the rigid connection. The deflection of the base plate is shown in Figure VII.9 and the close-up of the structure where maximum deflection occurs is shown in Figure VII.10

In order to determine the stress and the corresponding factor of safety, two different analyses are done. Firstly, the structure is optimized to have a factor of safety higher than 1.65, and secondly, the factor of safety for the hardware to be higher than 6. Accordingly, the reaction forces are determined at the bolt head under maximum stress and the factor of safety is determined using hand calculations and ASTM A193 Grade B16 Standard for a 3-inch diameter bolt. More explanation regarding the same is presented under the ”Bolt Analysis”.

The von Mises stress for the base plate design is shown in Figure VII.11 and a close-up of the maximum stress is shown in Figure VII.12. As expected, the maximum stress occurs at the bolt which is under most tension. As the plate tries to flip due to the applied loads, the fixed constraints on the bolt head try to stay in place hence warping the structure around the bolt head.

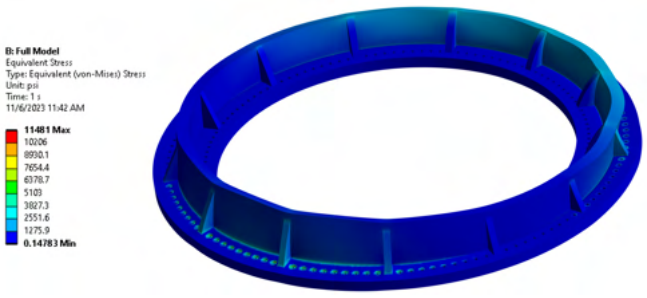

Fig. VII.11: Total Von Mises Stress (psi)

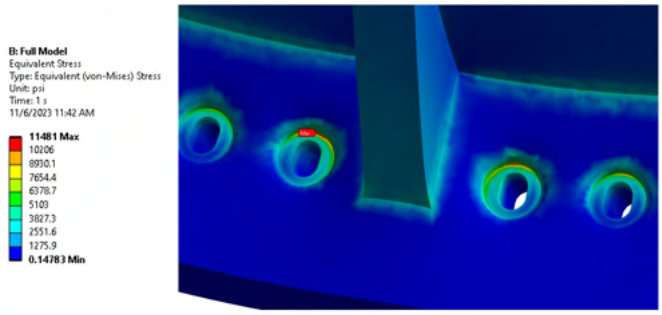

Fig. VII.12: Max Stress at the Bolt Head in Tension (psi)

A close-up of the maximum stress with a wire frame is also shown in Figure VII.13. Clearly, the maximum stress is not due to the warping of the element or singularity error however it occurs due to the warping of the structure itself as the tower tries to flip. This adds strength to the argument of having a good mesh.

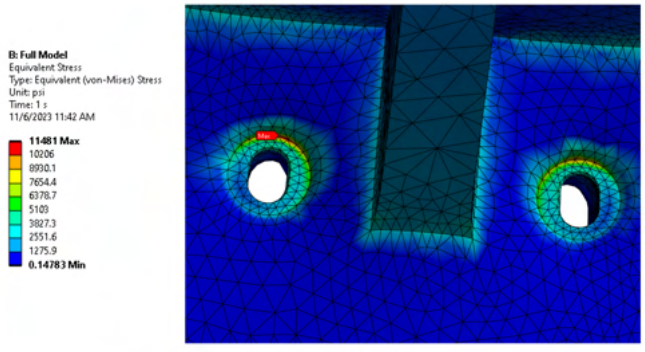

Fig. VII.13: Close up of the max stress with wireframe (psi)

Finally, the minimum factor of safety is determined to be 3.15 for the structure itself as shown in Figure VII.14. Since the maximum stress occurs at the bolt heads in tension, this minimum factor of safety also occurs around there. A close-up of this scenario is shown in Figure VII.15

Fig. VII.14: Factor of Safety

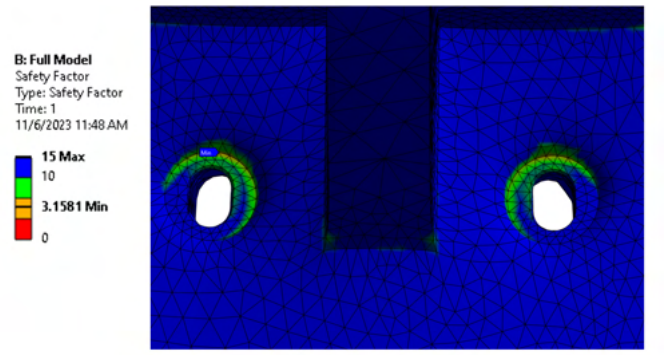

Fig. VII.15: Close up at the Lowest Factor of Safety around the Bolt Head in Tension

F. Weld Analysis At Areas of Interest

Since the base plate is going to be welded to the tower and the side supports are going to be welded to the base plate itself, it is important to ensure that the max shear stress around those boundaries has a considerable factor of safety for it to be welded. Accordingly, the shear stress is determined. A close-up of the max shear stress around the bolt head and two probes around the boundaries with maximum shear stress is shown in Figure VII.16 Although the design does not model the welds directly, the stress around these areas gives a good approximation of the stress in the welds. These areas will be fillet welded along all of the edges. The maximum sheer

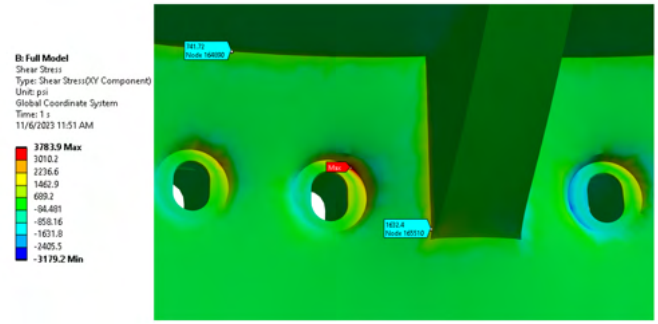

Fig. VII.16: Close up at the max shear stress (psi)

stress in the welds of the flange is 741 psi, and the maximum sheer stress in the welds of the angle brackets is 1632 psi. Using *Shigley's Mechanical Engineering Design*, the welding

strength of various welds are found and compared to these maximum stresses. Figure Figure VII.17 tabulates known data for the maximum allowable shear stress in various strength fillet welds. If an electrode number of E90 is chosen, the given

Schedule A: Allowable Load for Various Sizes of Fillet Welds

	Strength Level of Weld Metal (EXX)						
	60*	70*	80	90*	100	110*	120
	Allowable shear stress on throat, ksi (1000 psi) of fillet weld or partial penetration groove weld						
$\tau =$	18.0	21.0	24.0	27.0	30.0	33.0	36.0

Fig. VII.17: Allowable Sheer Stress for Fillet Welds *Shigley's Mechanical Engineering Design*

allowable sheer stress is 27 ksi as per tests done by the AISC-AWS committee. This source also suggests a factor of safety of 1.5 to account for fatigue loading which could be present in the case of a wind turbine design. The maximum shear stress found in the design of 1632 psi should be multiplied by this value to account for fatigue. To find the resulting factor of safety for the welds in the base, the allowable stress is divided by the maximum stress.

$$FS = \frac{\tau_{allowable}}{\tau_{actual}}$$
$$FS = \frac{27ksi}{(1.632 * 1.5)ksi} = 11$$

This value exceeds the specified factor of 6 necessary for all connections. Furthermore, to check the integrity of the weld metal itself, E90 welds have a tensile strength of 90 ksi as shown in figure Figure VII.18. The maximum von-misses

AWS Electrode Number*	Tensile Strength kpsi (MPa)	Yield Strength, kpsi (MPa)	Percent Elongation
E60xx	62 (427)	50 (345)	17–25
E70xx	70 (482)	57 (393)	22
E80xx	80 (551)	67 (462)	19
E90xx	90 (620)	77 (531)	14–17
E100xx	100 (689)	87 (600)	13–16
E120xx	120 (827)	107 (737)	14

*The American Welding Society (AWS) specification code numbering system for electrodes. This system uses an E prefixed to a four- or five-digit numbering system in which the first two or three digits designate the approximate tensile strength. The last digit includes variables in the welding technique, such as current supply. The next-to-last digit indicates the welding position, as, for example, flat, or vertical, or overhead. The complete set of specifications may be obtained from the AWS upon request.

Fig. VII.18: Electrode Strengths *Shigley's Mechanical Engineering Design*

stress found in the welded areas is found to be about 7 ksi. This yields a factor of safety well above 6. These calculations ensure that the welds in the base will be strong enough to handle the loading and resulting stress.

G. Bolt Failure Analysis

The bolts are modeled as a fixed support on an area around the bolt holes that represent a washer with a nut fixing it in place. This represents a bolt because if the bolt is working properly it will constrain any motion of the base around the area of the washer. In ANSYS, a reaction force probe is placed on the fixed constraint which is equal to the force that is transmitted to the bolt. The force in the y direction of this reaction force is used to analyze the stress in the bolt. Dividing this force by the cross-sectional area of the bolt yields the stress in the bolt and is compared to known bolt standards. An existing manufacturer, Nut, is chosen for this design because of their availability of large threaded studs for wind turbine applications and they provide specifications for their products. For the final design, a 3-inch ASTM A193 Grade B16 bolt[10] was chosen with a tensile strength of 110 Ksi. In the final design, the maximum bolt reaction force in the y direction is $1.21 * 10^5 lbf$ as shown in Table XI . Dividing this by the area of the 3 inch screw yields,

$$\sigma = \frac{1.21 * 10^5 lbf}{\pi * (1.5in)^2} = 17.1ksi$$

The factor of safety for this bolt is therefore,

$$FS = \frac{\sigma_{allowable}}{\sigma_{actual}}$$
$$FS = \frac{110ksi}{17.1ksi} = 6.4$$

This is greater than the required factor of safety for connections of 6 passing this requirement.

Direction	Reaction Forces (lbf)
X	13843
Y	-1.21e5
Z	-15945

TABLE XI: Reaction Forces at the Bolt Head Under Maximum Stress

VIII. Design time estimate

Topic	Hours Taken
Prior Research	3
Hand Calculations and Verification	10
Designing and Modelling	30
FEA Simulations	70
Post-Processing and Analysis	5
Compiling Results and Final Paper	25

TABLE XII: Rough Time Estimate for Each Aspect of the Design and Analysis.

REFERENCES

[1] *Matweb material data sheet*. [Online]. Available: https://www.matweb.com,
Annotation: Used for material properties.

[2] F. Bañuelos-Ruedas, C. Ángeles Camacho, and S. Rios-Marcuello, "Methodologies used in the extrapolation of wind speed data at different heights and its impact in the wind energy resource assessment in a region," *Wind Farm - Technical Regulations, Potential Estimation and Siting Assessment*, 2011. DOI: 10.5772/20669.

[3] U. S. E. P. Agency, *Renewable energy fact sheet: Wind turbines 2013*, 2023. [Online]. Available: https://nepis.epa.gov,
Annotation: Used to find the life expectancy of a wind turbine.

[4] E. d. Vries, *Haliade-x uncovered: Ge aims for 14mw*, Mar. 2019. [Online]. Available: https://www.windpowermonthly.com/article/1577816/haliade-x-uncovered-ge-aims-14mw.

[5] E. Toolbox, *Engineering toolbox*, 2023. [Online]. Available: https://engineeringtoolbox.com,
Annotation: Used to find equations for common engineering practice.

[6] NCEES, *Professional Engineer Mechanical Handbook*, 1.5. NCEES, 2023. [Online]. Available: https://help.ncees.org/article/87-ncees-exam-reference-handbooks,
Annotation: Used as a reference for various formulas, best practices, and material properties.

[7] ANSYS, *ANSYS Mechanical APDL Element Reference*, 14.0. ANSYS, Inc., 2012,
Annotation: Used as a reference for suitable element selection and keyoptions.

[8] ANSYS, *ANSYS Mechanical APDL Modeling and Meshing Guide*, 15.0. ANSYS, Inc., 2013,
Annotation: Used as a reference for modelling and meshing rules and reccomendations within APDL.

[9] R. Budynas and K. Nisbett, *Shigley's Mechanical Engineering Design*, 10th. McGraw Hill, 2014.

[10] B. B. Nut, *Astm a193 grade-b16 - bigboltnut.com*, 2023. [Online]. Available: https://www.bigboltnut.com/product/astm-a193-gr-b16.html,
Annotation: Used as a reference for standard bolt sizes.

[11] ANSYS, *Mechanical APDL Theory Reference*. ANSYS, Inc., 2013,
Annotation: Used as a reference to brush up on any relevant theories, or to obtain clarification on the methods used by Ansys APDL.

[12] I. ANSYS, *Ansys meshing user's guide*, Release 13.0, Canonsburg, PA, 2023. [Online]. Available: https://www.ansys.com/,
Annotation: Used as a reference for meshing rules and reccomendations within Workbench.

[13] B. McGinty. "Stress concentrations at holes." Accessed on October 7, 2023. (2023), [Online]. Available: https://www.fracturemechanics.org/hole.html.
Annotation: Used as a reference for stress concentrations about holes.

APPENDIX A
ENGINEERING DRAWING FOR TOWER

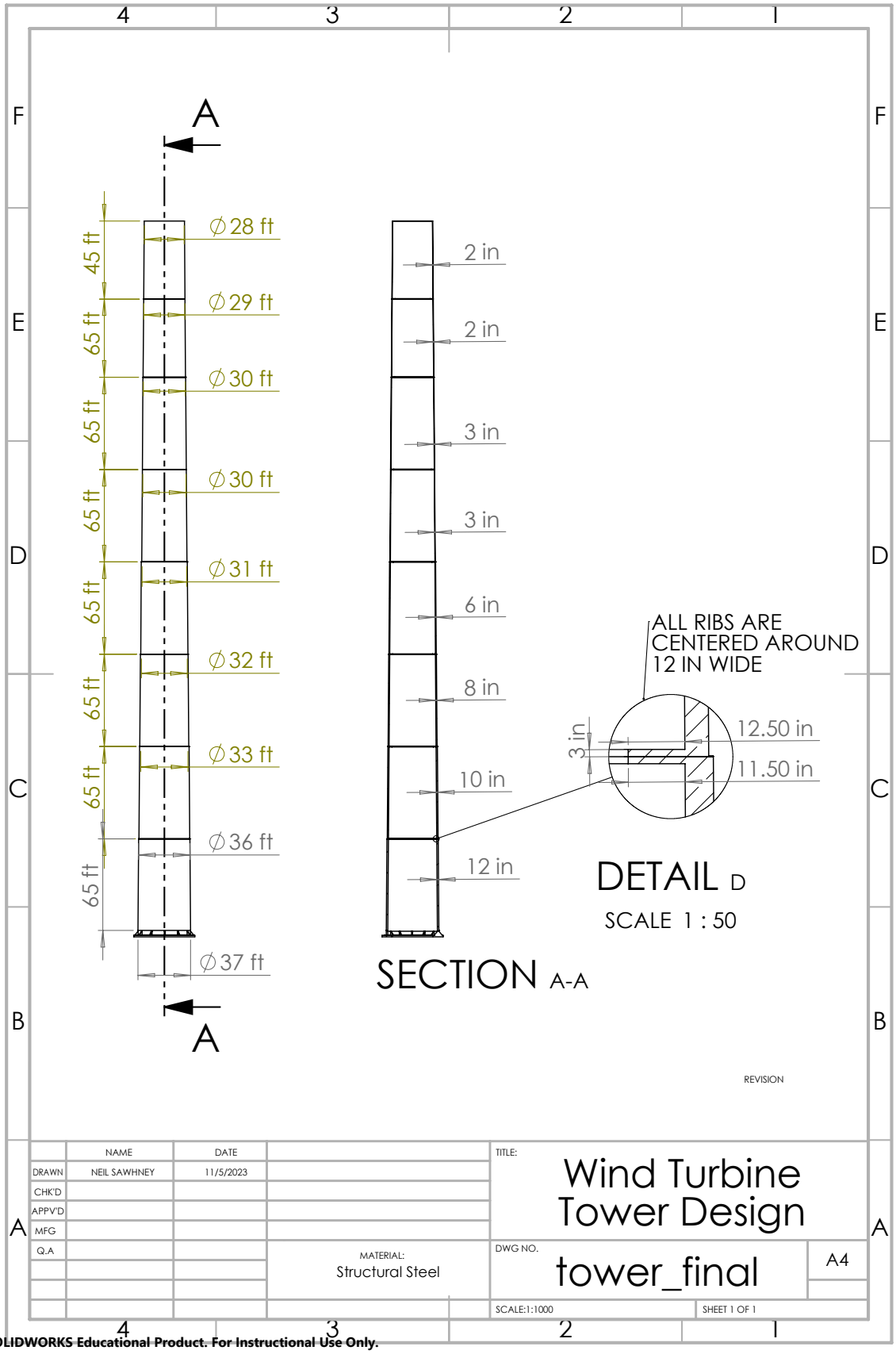

APPENDIX B
ENGINEERING DRAWING FOR BASE

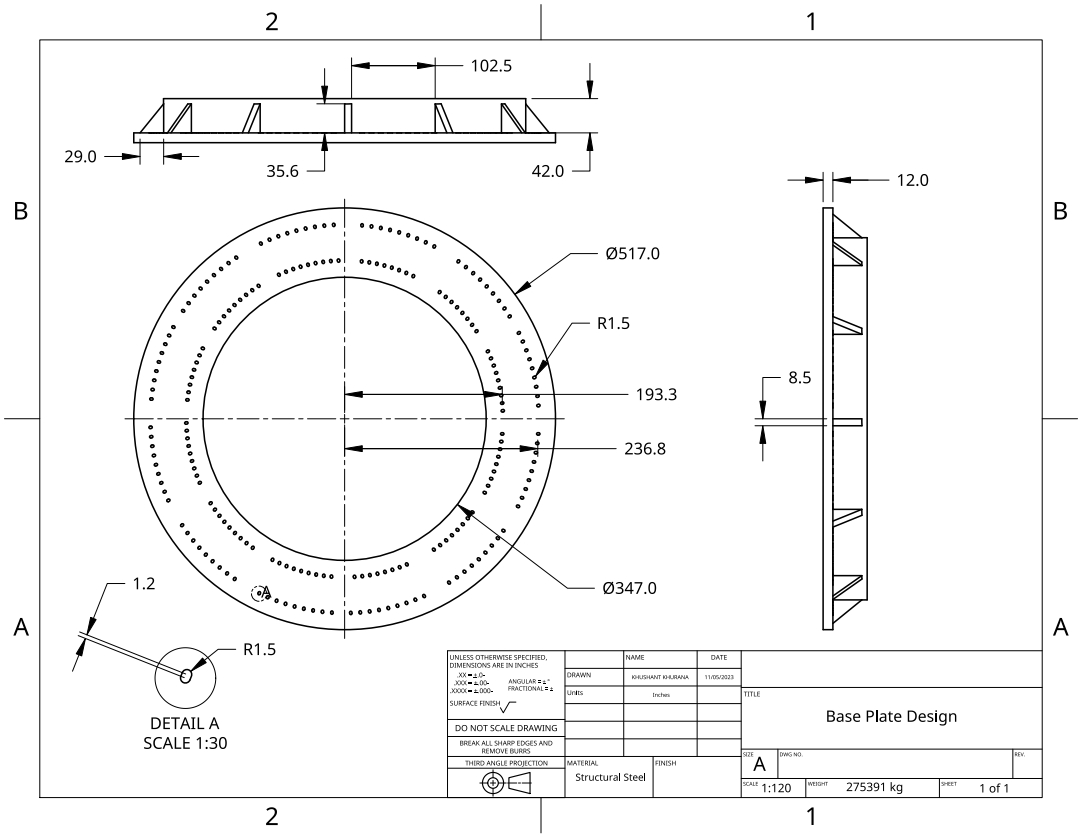

(a) Detailed Sketch of the Base Plate Design

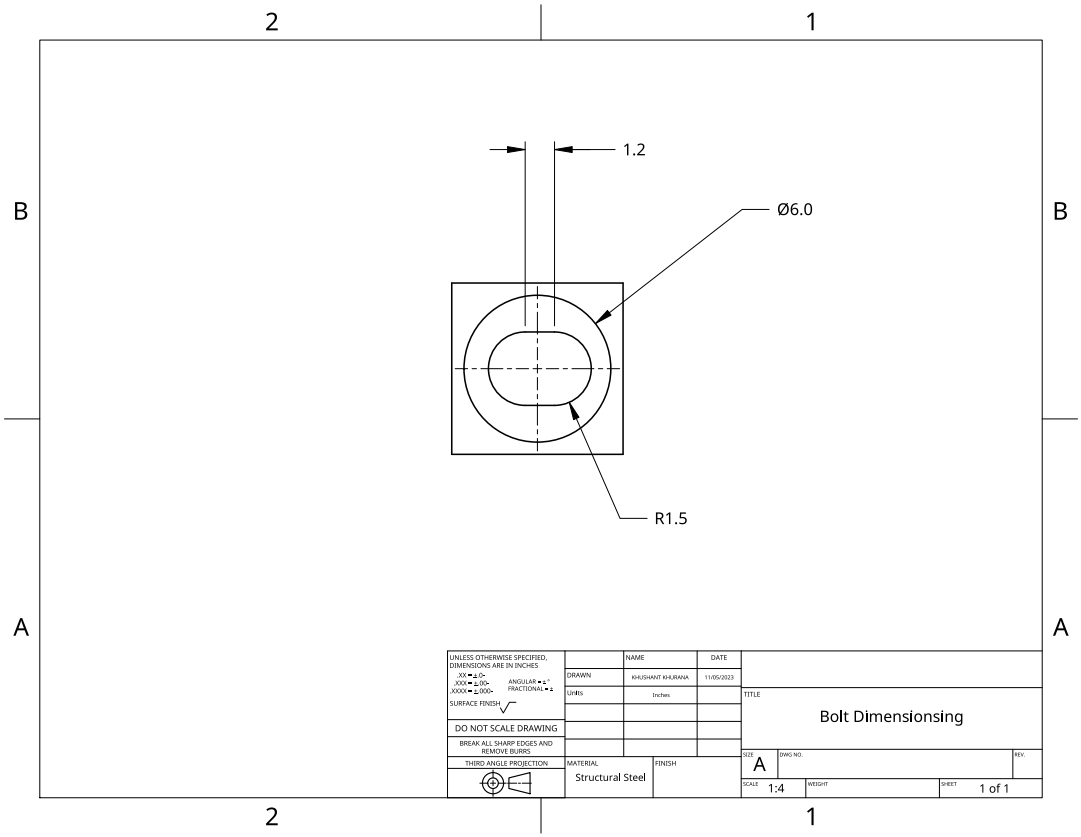

(b) Detailed Sketch of the Bolt Design

APPENDIX C
DISCARDED FEATURES

A. Tower Eccentricity

The eccentricity of the tower was initially included as a parameter during the optimization process. However, it became apparent that although the eccentricity helps to offload some of the nacelle's weight, it tends to worsen the effect of a perpendicular wind load. For this reason, eccentricity was fixed at a perfect circle for the remainder of the analysis.

B. Tower Base Filleting

In addition to analyzing the tower's gradual thickening, tower base filleting was analyzed as shown in Figure C.1. The motivation is the same as the thickening approach, to decrease the stress concentrated at the very bottom of the structure.

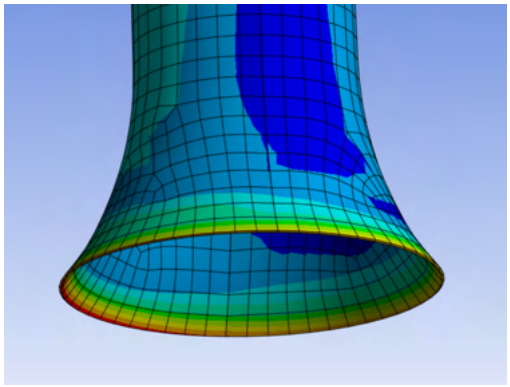

Fig. C.1: The bottom base of the tower with a fillet_width of 5 ft

Since increasing the width of the entire structure leads to a dramatic decrease in maximum stress, it was theorized that increasing the width only at the very bottom through the use of a fillet would have the benefits of increasing the entire width without using so much extra material. However, as shown in Figure C.2, increasing the width of the fillet actually leads to an increase in maximum stress and deformation.

P33 - fillet_width	P20 - Equivalent Stress Maximum	P21 - Total Deformation Maximum
ft	Pa	m
5	1.4933E+08	0.52072
10	1.5578E+08	0.52404
15	1.691E+08	0.53802
20	1.9786E+08	0.56707
25	1.8533E+08	0.63524

Fig. C.2: Max stress and max deformation with increasing fillet radius

These results made it clear that tower gradual thickening was the better method.

C. Single Layer of Bolts for Base Plate

The first model that is designed for the base included one layer of bolts with 52 bolts. These bolts are designed to be 6 inches in diameter and there are 52 instances. As shown in

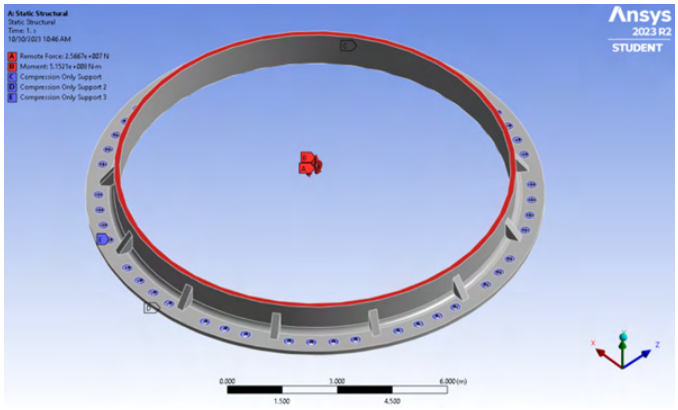

Fig. C.3: Constraints applied

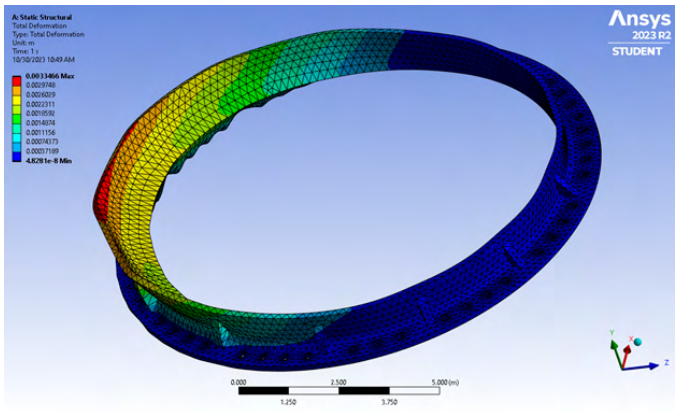

Fig. C.4: Initial Deflection (m)

Figure C.5 and Figure C.6 There is a very low factor of safety indicating that this design should be improved.

The next simulation that is performed to improve the results included around 100 bolts to try to secure the base more, but the bolts are decreased in size to 2 inches because of the practical feasibility of securing such bolts. The previous design had 6-inch bolts which are not common in wind turbine designs. In this interaction, the mesh is also improved. As can be seen in Figure C.5 the previous mesh is not very fine. In particular, there are only two nodes across the width of the flange and along each of the brackets. The holes themselves also have minimal nodes and can be improved as well. The results of the finer mesh and increased bolt numbers are shown in Figure C.8 and Figure C.7. The mesh size is now 2-3 inches for the body, and 0.5 inches for the bolt holes, and the factor of safety is now 1.57 for the flange. This is clearly an improvement from the previous design, but it is still not good enough. In addition, the stress in the bolts is around 100 ksi which is close to the tensile strength without any factor of safety. Because of these results, a different design methodology is proposed.

D. Two Layer of Bolts for the Base Plate

It is decided to try a base plate with two layers of bolts on the outer edge. For these simulations, the same 2-inch bolt size is used. This simulation has slightly better results, but the bolt

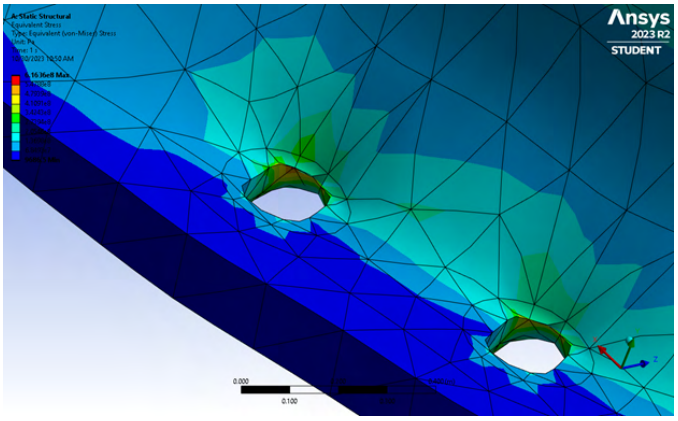

Fig. C.5: Total Von Mises Stress (Pa)

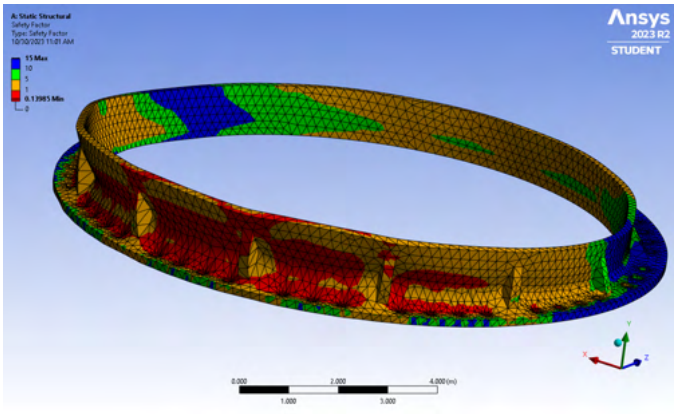

Fig. C.6: Initial Factor of Safety

is still failing its factor of safety requirement. It can be seen in figure that the outer layer of bolts is really not contributing so much to the overall design and the inner ring of bolts is taking all of the stress. Because of these conclusions, the second ring of bolts is moved to the inside of the flange so that it could help take more of the load. This ended up being the final design that worked and is discussed earlier in the paper. A high factor of safety in the structure is achieved in this design, and using 3-inch bolt studs, a high factor of safety for the bolts is also achieved.

E. Vertical Beams and Cross Beams

One design choice that was discarded during the optimization process was cross beams and vertical beams in the interior of the wind turbine shaft. The chosen design parameters were as follows:

1) An eccentricity of 1
2) A bottom and top width of 35 and 33.25 feet respectively (draft ratio of 0.95)
3) Constant thickness of 10 inches for shaft

This design is then compared with and without the internal beaming. The internal beams for this design are given a rectangular tube cross-section with a width of 9.8 inches, and a thickness of 4 inches. The chosen number of internal cross beams per section is 3 (a total of 18 beams) with an equal

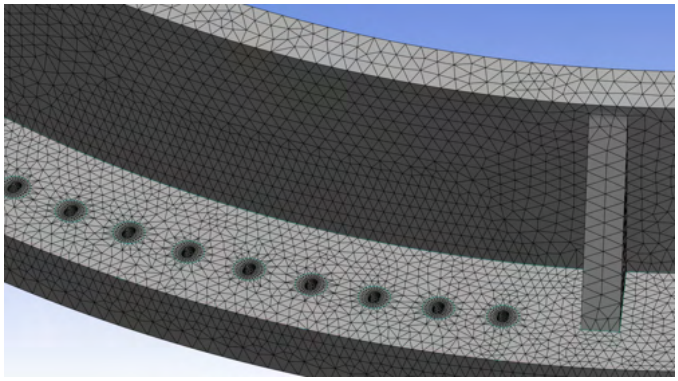

Fig. C.7: Mesh of Updated Design

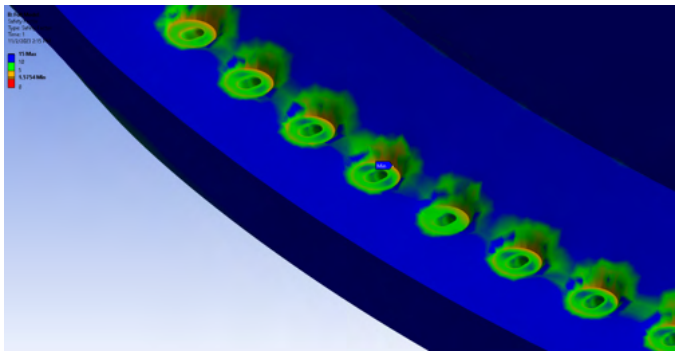

Fig. C.8: Factor of Safety Updated Design

angle of 120 degrees between each. For the beam structure, crossbeams are placed in closer intervals towards the top as most of the forces act on the top of the turbine shaft, so more support is needed in those areas. Vertical beams are added to give the shaft extra support. Like the fully optimized design, the wind turbine shaft is modeled as a two-dimensional shell element with the beams modeled as one-dimensional elements.

The mesh for this design (referred to as version 1) is shown in Figure C.13 and Figure C.14.

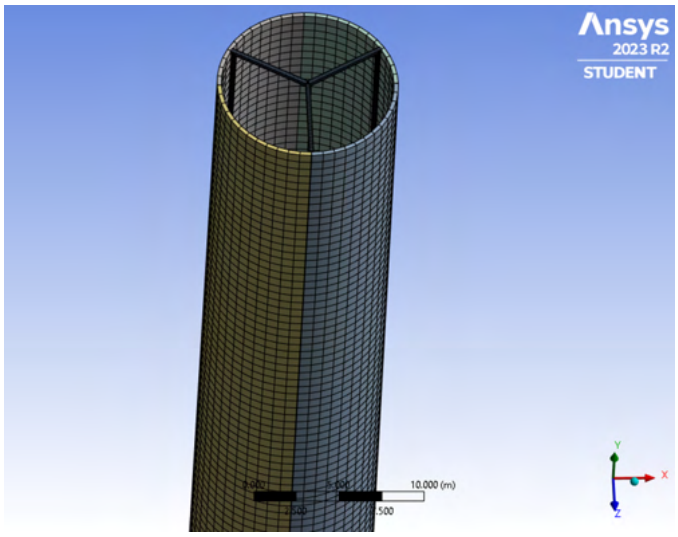

Fig. C.14: Meshing for Wind Turbine Shaft

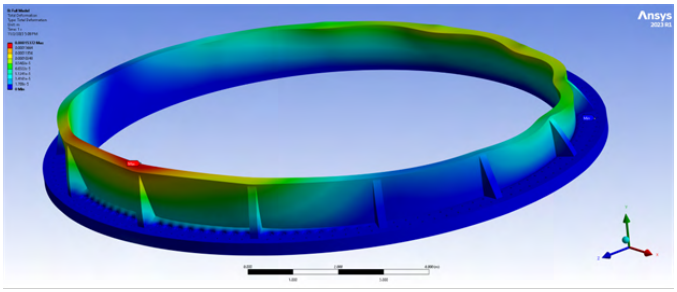

Fig. C.9: Deflections Stress in Two Layers of Bolts Base Plate (m)

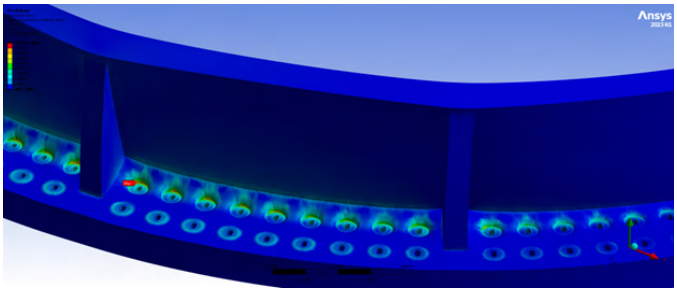

Fig. C.10: Stress in Two Layers of Bolts Base Plate

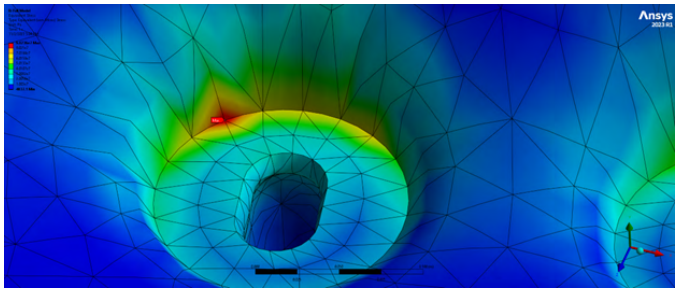

Fig. C.11: Zoomed In Max Stress in Two Layers of Bolts Base Plate

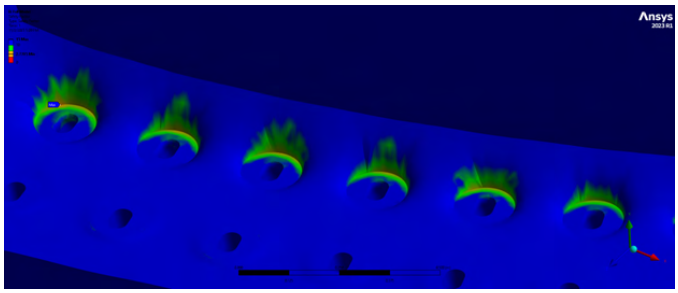

Fig. C.12: Factor of Safety for Two Layers of Bolts Base Plate

As mentioned before, to see if the beam elements have a substantial effect on the system, both the shaft with and without the beams are modeled and simulated under all the structural constraints, forces, pressures, and moments.

First, the turbine shaft is modeled without the internal beams. The total deformation and von Mises stresses are simulated for this case, as shown in Figure C.15, Figure C.16 and Figure C.17.

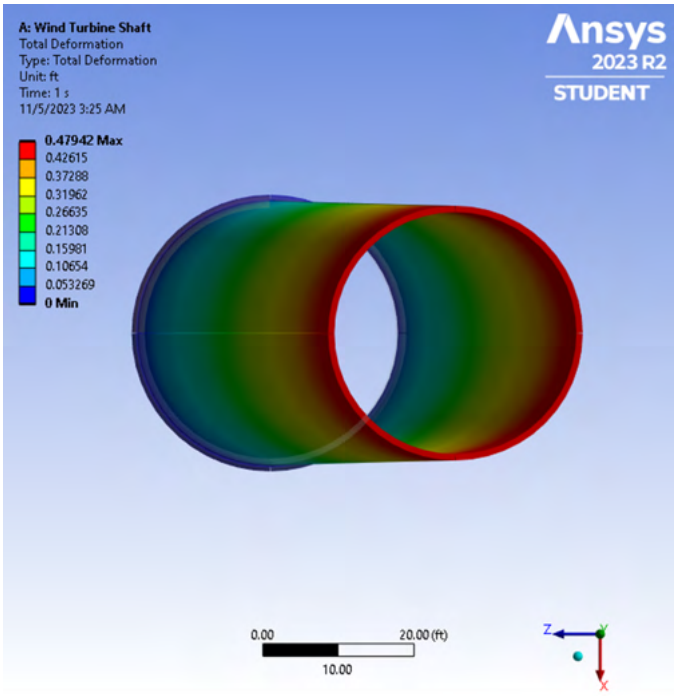

Fig. C.15: Total Deformation, No Beams - Top View)

Figures Figure C.18,Figure C.19, and Figure C.20 show the deformation and stress concentration of the turbine shaft with the vertical and cross beams included [Version 1].

Figures Figure C.21, Figure C.22, and Figure C.23 show another scenario [Version 2], with a larger beam cross section (width of 19.75 inches and thickness of 1.975 inches):

To summarize, the maximum deformation for the turbine shaft without the beams is 0.479 ft, 0.474 ft for version 1, and 0.468 ft for version 2. The difference in deflection is therefore considered to be negligible. Even with the largest case (version 2) the difference in deflection is around a tenth of an inch while adding around 900,000 lbs of material. Because of this, we chose to avoid the vertical beam and cross beams in our final design.

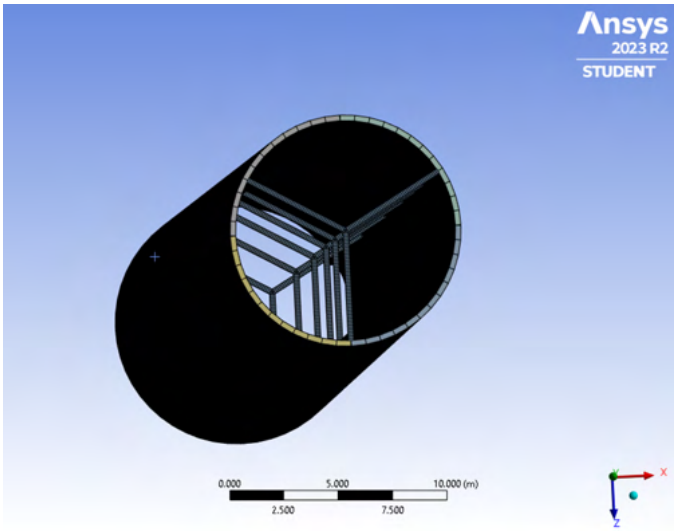

Fig. C.13: Meshing for Internal Beams

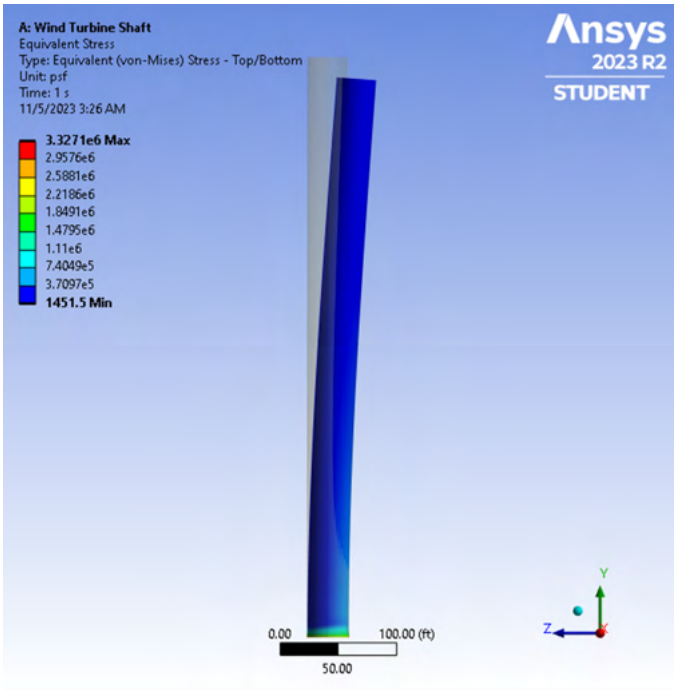

Fig. C.17: Von Mises Stress, No Beams

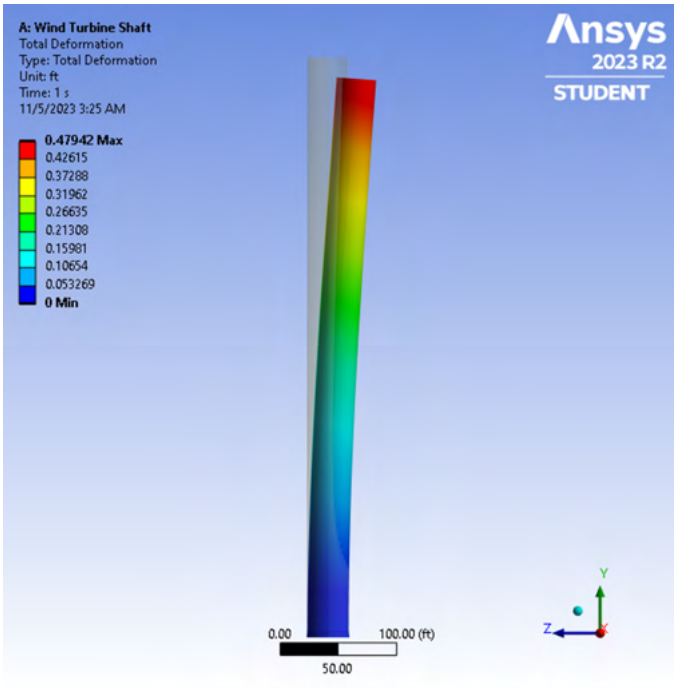

Fig. C.16: Total Deformation, No Beams - Side View)

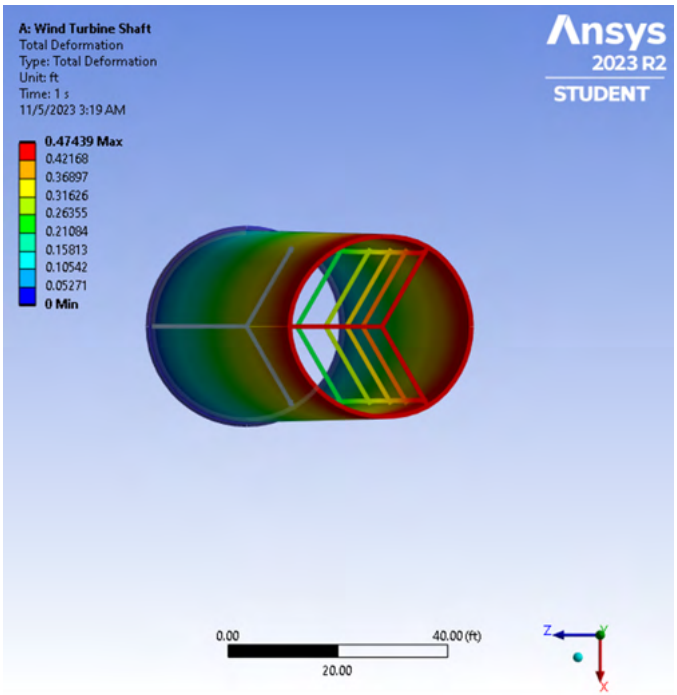

Fig. C.18: Total Deformation, Beams Included (Version 1 Top View)

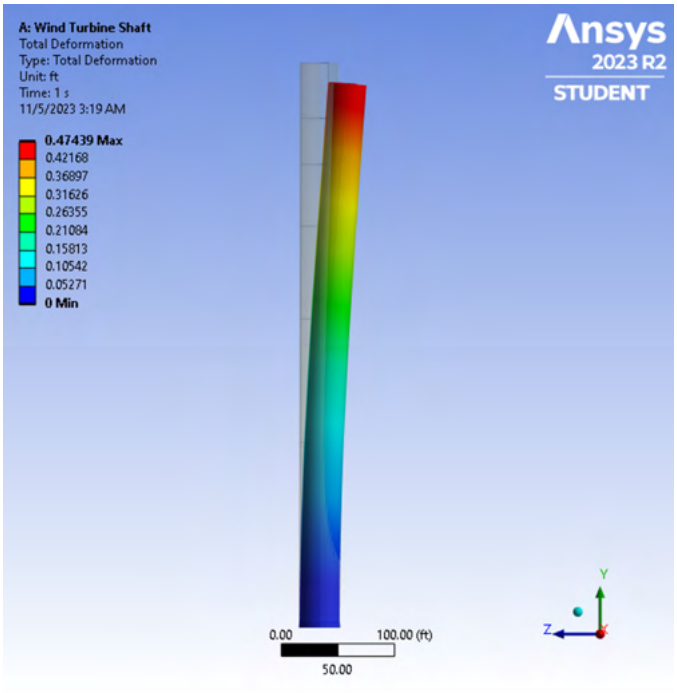

Fig. C.19: Total Deformation, Beams Included (Version 1 - Side View)

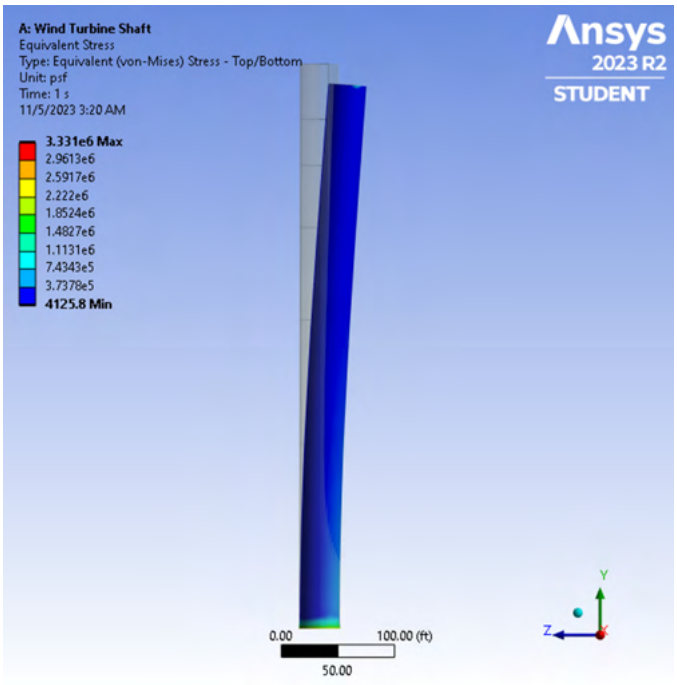

Fig. C.20: Von Mises Stress, Beams Included (Version 1 - Side View)

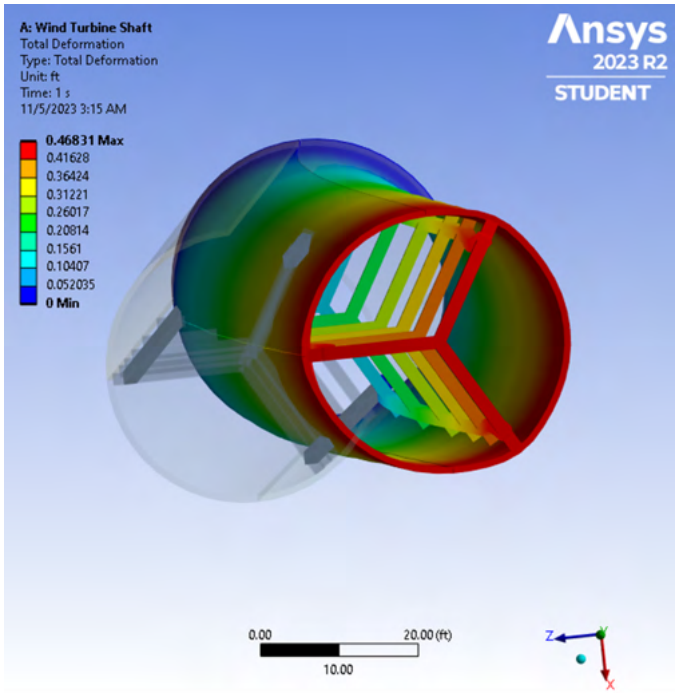

Fig. C.21: Total Deformation, Beams Included (Version 2 - Side View)

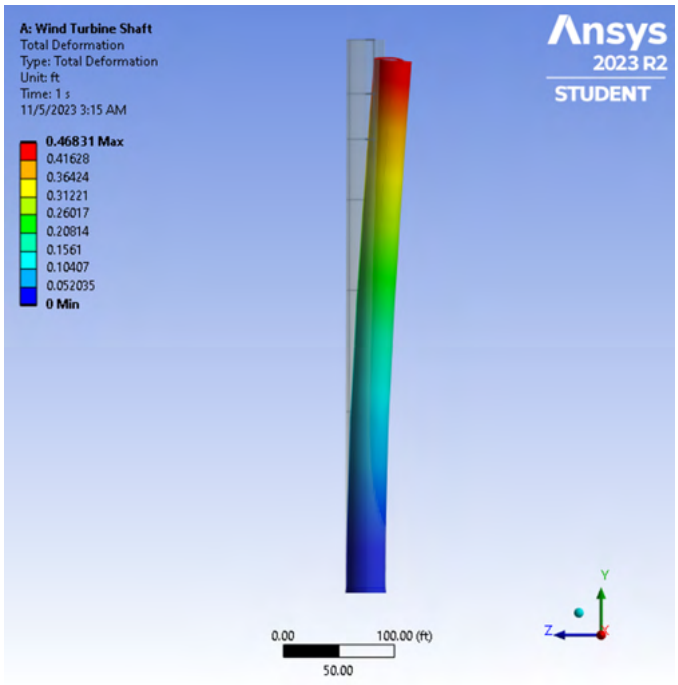

Fig. C.22: Total Deformation, Beams Included (Version 2 - Top View)

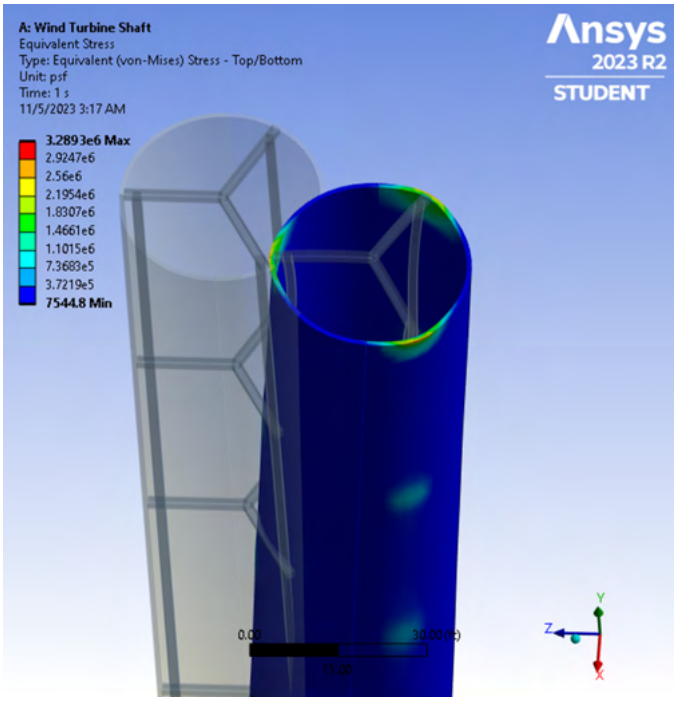

Fig. C.23: Von-Misses Stress, Beams Included (Version 2)